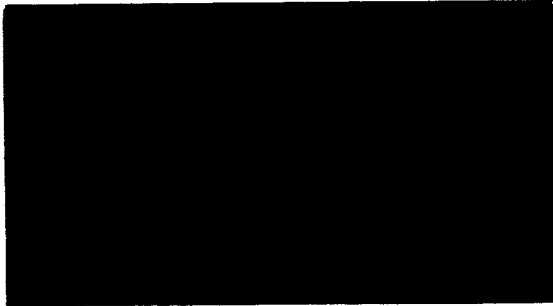GPO PRICE $ _____

CFSTI PRICE(S) $ _____

Hard copy (HC) _____ 2.00

Microfiche (MF) _____ .75

ff 653 July 65

HEAT
TECHNOLOGY
LABORATORY
INC.
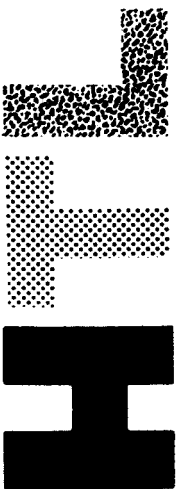
4308 Governors Drive - Huntsville, Alabama - 35805

FINAL REPORT
CONTRACT NAS8-11850
Vol. I
SATURN BASE FLOW STUDIES

Compiled By

W. W. Youngblood

HEAT TECHNOLOGY LABORATORY, INC.
Huntsville, Alabama

HTL-TR-22

October 14, 1965

Prepared For

National Aeronautics and Space Administration
George C. Marshall Space Flight Center
Huntsville, Alabama

CONTENTS

CONTENTS (Con't.)

CONTENTS (Con't.)

ABSTRACT   23836

An investigation was made of various problem areas re-
lated to the definition of the base flow environment of
SATURN vehicles. This investigation included studies of:
(1) Integration Procedures in the Method of Characteristics
for a Reacting Gas, (2) Multiple Combustion Products Freezing
Point Determination, (3) Effect of Passage Through a Shock
Wave on the Properties of a Reacting Gas, (4) Specific Heat
Variation Through a Normal Shock, (5) The Applicability of
Latvala's Method of Circular Arcs for Predicting SATURN
Plume Boundaries, (6) Determination of Velocities in a
Turbulent Gas Stream from Scattering of a Monochromatic
Light Beam, and (7) Importance of Turbulence Intensity on
the Base Heating Problem.

SUMMARY

An investigation was made of various problem areas
related to the definition of the base flow environment of
SATURN vehicles. The results of the investigation are sum-
marized below.

Part I - Integration Procedures in the Method of
Characteristics for a Reacting Gas. - An investigation was
made to determine the variation from one-dimensionality that
exists when using the one-dimensional form of the chemical
kinetics equations to describe a two-dimensional flow by the
method of characteristics. It was concluded that an accurate
determination of the variation requires that a complete method
of characteristics solution be made of flow throughout the
entire nozzle and a comparison be made with values obtained
using one-dimensional flow equations.

Part II - Multiple Combustion Products Freezing Point
Determination. - An evaluation was made of various simplified
methods of treating the chemical kinetics of reacting gas flows
through the use of freezing point determinations of the chemical
reactions. It was concluded that the limitations associated
with the various simplified methods were not justified by
computation time savings over a complete nonequilibrium solution.

Part III - Effect of Passage Through a Shock Wave on the Properties of a Reacting Gas. - An investigation was made of the suitability of various methods for computing flow parameters and compositions of reacting gases flowing through shock waves. Sample computations were made for the following two assumptions: (1) frozen composition through the shock, and (2) equilibrium composition through the shock. For method-of-characteristics solutions based upon conditions following a shock wave, the calculated properties of the gas obtained from the assumption of equilibrium composition more closely represented the actual values than the results obtained for the frozen composition assumption.

Part IV - Specific Heat Variation Through a Normal Shock. - A method is outlined for the determination of the variation of the specific heat through a normal shock wave using partition functions and temperature profiles. Recommendations are made for the possible solution of this problem by using experimentally determined temperature profiles and relaxation times.

Part V - The Applicability of Latvala's Method of Circular Arcs for Predicting SATURN Plume Boundaries. - A comparison of plume boundaries predicted by Latvala's Method of Circular Arcs with photographs of the SATURN SA-1 exhaust plume shows that Latvala's Method gives good agreement with observed SATURN plume shapes at altitudes up to about 24 Km and above about 50 Km.

Part VI - Determination of Velocities in a Turbulent
Gas Stream From Scattering of a Monochromatic Light Beam. -
An analytical method was developed to determine mean flow

velocity and turbulence intensity from measurements of Doppler

shift and broadening of a monochromatic light beam scattered

from smoke particles suspended in a turbulent gas stream.

The application of this analysis to a representative set of

data showed that this method can in principle be used for

accurate measurements of turbulent gas stream velocities.

Part VII - Importance of Turbulence Intensity on the
Base Heating Problem. - A high degree of turbulence intensity

has been observed in the base region of model tests experiencing

supersonic flow. The influence of turbulence intensity on

convective heat transfer to the base can be qualitatively

predicted if Richardson's empirical equation is used. The

difficulty of quantitative prediction is due to the lack of

a satisfactory method to relate the turbulence intensity to

the critical Reynolds number.

PART I

INTEGRATION PROCEDURES IN THE METHOD

OF CHARACTERISTICS FOR A REACTING GAS

By

Beverly J. Audeh

INTRODUCTION

The analysis of chemically reacting gas flow fields may be accomplished by including the chemical kinetic equations in the method of characteristics. The chemical kinetic equations are usually integrated along streamlines using the one-dimensional form of the equations. An investigation was made to determine the error involved in using the one-dimensional form of the chemical kinetic equations to describe a two-dimensional flow field.

LIST OF SYMBOLS

c Velocity of sound

g Gravitational constant

h Specific enthalpy

J Mechanical energy equivalent of heat energy

k_f, k_b Specific reaction rate constants, forward reactions and reverse reactions

n Total number of reactions

p Pressure

q Speed

t Slope of a streamline

u Velocity component in x direction

v Velocity component in y direction

x Distance coordinate

y Distance coordinate

α'_{ij}, α''_{ij} Stoichiometric coefficient of the i th species in the j th reaction, reactions and products respectively

γ Ratio of specific heats

ζ Reaction parameter in axisymmetric flow.

η Axis normal to streamline

θ Angle of inclination of the streamline relative to axis of symmetry

ξ Axis along streamline

ρ Density

σ Concentration: mass fraction divided by molecular weight.

Subscripts:

i Index

j Index

k Index

n_r Number of reactions

DISCUSSION

The calculation of flow properties of a chemically reacting gas through a two-dimensional nozzle can be accomplished by application of the method of characteristics including chemical reaction equations. This calculation requires the integration of the chemical kinetic equations along streamlines. In order to integrate these equations, approximations are made to reduce the flow equations to one-dimensional form along the streamlines.

These approximations reduce the following set of Equations (1-3) in two-dimensional form (Ref. 1):

Energy:

$$\frac{1}{\rho}\frac{\partial \rho}{\partial \xi} - \frac{g}{\gamma P}\frac{\partial P}{\partial \xi} - \sum_{j=1}^{n}\left[\frac{h_j g J(\gamma-1)}{C^2} - \frac{1}{\sum_i \sigma_i}\right]\frac{\partial \sigma_k}{\partial \xi} = 0 \quad (1)$$

Momentum:

$$q\frac{\partial q}{\partial \xi} = -\frac{g}{\rho}\frac{\partial P}{\partial \xi} \quad (2)$$

Continuity:

$$\frac{\partial \sigma_k}{\partial \xi} = \frac{\zeta k}{\rho q} \quad (3)$$

where

$$\frac{\partial}{\partial \xi} = \frac{u}{q}\frac{\partial}{\partial x} + \frac{v}{q}\frac{\partial}{\partial y}$$

and

$$\zeta_k = \sum_{j=1}^{n_r} (\alpha''_{kj} - \alpha'_{kj}) \left[k_{fj} \prod_{i=1}^{n} (\rho\sigma_i)^{\alpha'_{ij}} - k_{bj} \prod_{i=1}^{n} (\rho\sigma_i)^{\alpha''_{ij}} \right]$$

to the set of Equations (4-6) in one-dimensional form:

Energy:

$$\frac{1}{\rho}\frac{\partial\rho}{\partial x} - \frac{g}{\gamma p}\frac{\partial p}{\partial x} - \sum_{j=1}^{n} \left[\frac{h_j g J(\gamma - 1)}{C^2} - \frac{1}{\sum_i \sigma_i} \right] \frac{\partial \sigma_i}{\partial x} = 0 \qquad (4)$$

Momentum:

$$q\frac{\partial q}{\partial x} = -\frac{g}{\rho}\frac{\partial p}{\partial x} \qquad (5)$$

Continuity:

$$\frac{\partial \sigma_j}{\partial x} = \frac{\zeta_j}{\rho q}\sqrt{1+t^2} \qquad (6)$$

where

$$t = \tan\theta$$

The degree to which Equations (4-6) represent an actual two-dimensional flow depends on the uniformity of the flow. From the equations, this implies that

$$\frac{\partial}{\partial \xi} = \frac{u}{q}\frac{\partial}{\partial x} + \frac{v}{q}\frac{\partial}{\partial y}$$

and

$$\frac{\partial}{\partial \eta} = -\frac{v}{q}\frac{\partial}{\partial x} + \frac{u}{q}\frac{\partial}{\partial y}$$

approach

$$\frac{\partial}{\partial \xi} = \frac{\partial}{\partial x}$$

and

$$\frac{\partial}{\partial \eta} = 0$$

This is approximately correct if v/q is negligibly small and $\frac{\partial}{\partial y}$ of p, ρ, σ or q is negligibly small. These conditions are required for the flow within the finite interval of operation of the method of characteristics from one point to the next along a streamline to approach one-dimensional flow. For long slender nozzles the one-dimensional representation is nearly correct. For short rapidly expanding flows where large flow inclinations along streamlines are involved, the one-dimensional representation may not be appropriate.

Within the method of characteristics the flow equations are applied along a particular streamline rather than over the entire flow area, hence the inclination of the streamline determines the accuracy of using the one-dimensional form of the equations.

In Ref. 1, the variable t is introduced to partially compensate for the two-dimensionality of the flow. In Eq. (6)

the arc length of the streamline is approximated by the chord length (Fig. 1). The variable t is a measure of the variation of the streamline from one-dimensional form. The amount of variation from actual one-dimensionality enters at each calculation of a point throughout the characteristic net. An absolute determination of the total variation requires a complete calculation over the entire nozzle and a comparison with values obtained using one-dimensional flow equations.

Equilibrium flow is a special case of a reacting gas flow. Der (Ref. 2) treats equilibrium flow through an axisymmetric expansion nozzle. Variation of velocity, degree of dissociation, pressure, temperature, and frozen Mach number across the nozzle-exit exists even though one-dimensional chemical kinetic equations were used within the calculation.

CONCLUSIONS

Two-dimensional flows approach one dimensionality in the limiting case. Solution by the method of characteristics, however, is based upon a finite difference technique which does not reach the limiting case. The amount of variation from actual one-dimensionality enters into the calculation at each point and affects the following points throughout the characteristic solution for a two-dimensional flow. An absolute determination of the total variation requires

a complete calculation over the entire nozzle and a comparison with values obtained using one-dimensional flow equations.

REFERENCES

1. Sarli, V. J., "Investigation of Nonequilibrium flow Effects in High Expansion Nozzles", United Aircraft Corp., Conn., September 20, 1963, N64-11743.

2. Der, J. J., "Theoretical Studies of Supersonic Two-Dimensional and Axisymmetric Nonequilibrium Flow, Including Calculations of Flow Through a Nozzle", NASA TR R-164, December 1963.
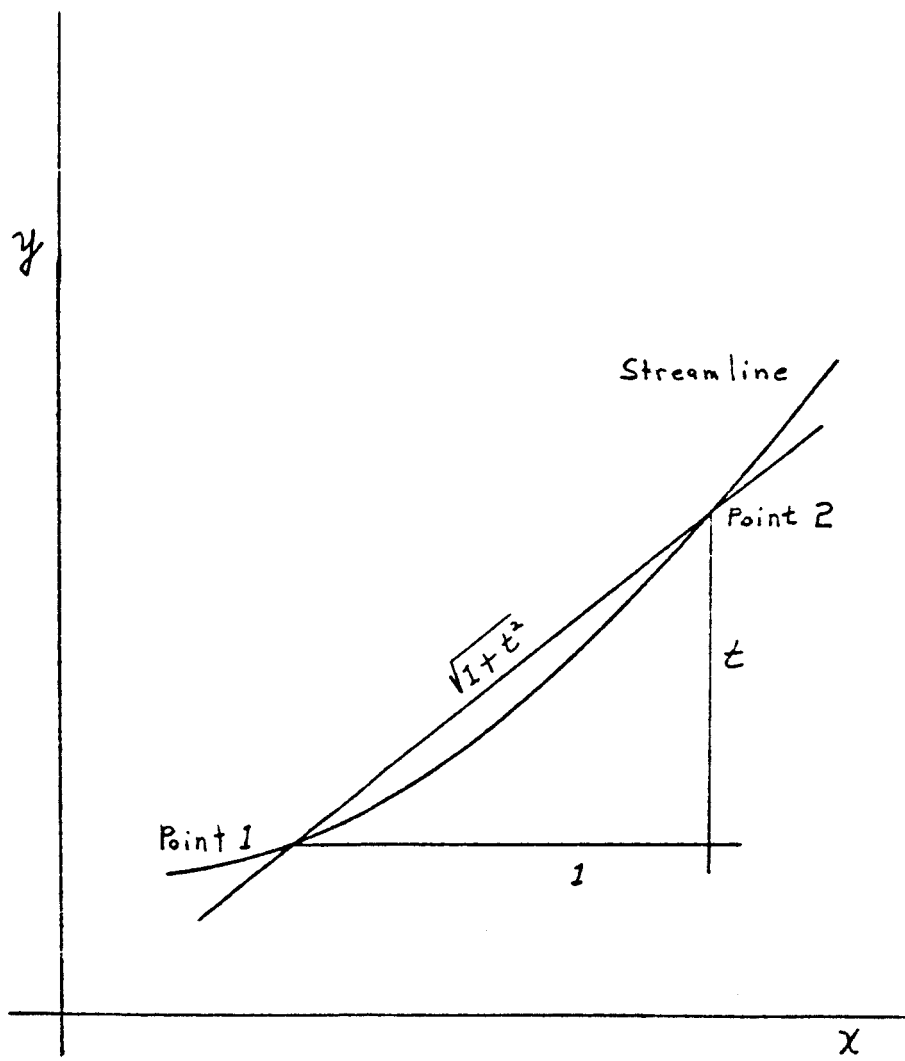
FIGURE 1. LINEAR APPROXIMATION OF A STREAMLINE

PART II

MULTIPLE COMBUSTION PRODUCTS

FREEZING POINT DETERMINATION

By

Beverly J. Audeh

INTRODUCTION

The exact description of a reacting gas flow requires complete evaluation of the coupled flow equations and chemical process equations. For single reactions (Ref. 1, 2, and 3) it has been possible to compute a freezing point as a result of local conditions changing so rapidly due to nozzle expansion that the reaction can not keep pace with the changes. Calculation of the conditions in the nozzle downstream of the freezing point is greatly simplified since the gas is treated as if it were of fixed composition through the rest of the nozzle. When multiple reactions are considered, the complexity of the combined and coupled chemical reactions makes definition of an accurate single freezing point difficult since each reaction has a different freezing point. An investigation was made to determine the accuracy limitations and the computation time savings resulting from the use of freezing point determinations in complex reacting flow.

DISCUSSION

The Bray Method

The Bray method (Refs. 4 and 5) to find the freezing point for complex reacting flow is based upon a check of each

reaction at every step of the calculation for freezing. Application of this method requires knowledge of the effect of each reaction on all the others. For complicated flow with many reactions this can become a ponderous task. Overall flow quantities (Ref. 6) obtained by the Bray method are comparable to those obtained using an exact finite rate nonequilibrium solution. Concentrations are, nevertheless, not as accurately predicted and the values can be used only qualitatively. A further restriction that the number of reactions involved must not exceed the number of chemical species less the number of elements involved in the flow, limits the cases to which the Bray method can be applied.

The Controlling Reaction Method

Another approach to determination of the freezing point of a complex flow is to assume that the chemical action of the gas mixture is controlled by only one of the reactions. This method (Ref. 7 and 8) implies that the entire flow can be treated as frozen as soon as the controlling reaction becomes frozen. If there is a single controlling reaction and if that reaction is judiciously chosen to determine the freezing point, this technique leads to a close approximation of the actual flow process. Assumption of a controlling reaction in the process does allow elimination of some species and their reactions on the basis of small equilibrium concentration. The choice of the correct controlling reaction requires

extensive a priori knowledge of the flow which in many cases is not available.

The Nonequilibrium Solution

Since both of the above techniques usually require a nonequilibrium solution in the initial stages, all necessary data for a complete nonequilibrium solution usually are available. With the application of modern digital computers, a nozzle flow calculation for exact nonequilibrium kinetic solution does not require excessive computer time. One example (Ref. 9) of the calculation through the diverging section of a nozzle required about 10 minutes of IBM 7090 time. Another case (Ref. 10), in which the flow was calculated from the combustion chamber through the converging section and the diverging section of the nozzle to the exit, required a total of 2 hours of IBM 7090 machine time. The greater part of this time, 1-3/4 hours, was used in computation of the flow field up to the throat. The computation through the divergent, supersonic portion of the nozzle requires a considerably shorter time than the convergent, subsonic portion and the critical throat section. While there is relatively small effect on nozzle performance (Ref. 11) because of the slow change in properties in the last part of the divergent supersonic nozzle, exact nonequilibrium solutions can be obtained in reasonable computer times without the limitations inherent in freezing point solutions.

An exact nonequilibrium solution for use with an existing nozzle is outlined in Ref. 12. Since the exact nonequilibrium solution is within reasonable time requirements, the assumptions and restrictions of freezing point calculations can be avoided by using the exact solution in supersonic nozzle flow analysis.

CONCLUSIONS

Evaluation of the method outlined by Bray and the method of a single controlling reaction to determine an effective freezing point indicates that the limitations on accuracy resulting from the use of these techniques are not usually warranted by computer time savings over the application of the exact nonequilibrium solution throughout the nozzle.

REFERENCES

1. Bray, K.N.C., Fourth AGARD Combustion and Propulsion Colloquium, pp. 279-285, Pergamon, 1961.

2. Nagamatsu, H.J. and Sheer, R.E., Jr., "Vibrational Relaxation and Recombination of Nitrogen and Air in Hypersonic Nozzle Flows", General Electric Research Laboratory Report No. 63-RL-(3429C), September 1963.

3. Stollery, J.L. and Park, C.,"Computer Solutions to the Problem of Vibrational Relaxation in Hypersonic Nozzle Flows", Imperial College of Science and Technology, Report No. 115, January 1963.

4. Bray, K.N.C. and Appleton, J.P., "Atomic Recombination in Nozzles: Methods of Analysis for Flows with Complicated Chemistry", University of Southampton, A.A.S.U. Report No. 166, April 1961.

5. Bray, K.N.C. and Appleton, J.P., "Atomic Recombination in Nozzles: Method of Analysis for Flows with Complicated Chemistry II", University of Southampton, A.A.S.U. Report No. 178, May 1961.

6. Bray, K.N.C., "Chemical Reactions in Supersonic Nozzle Flows", Ninth Symposium (International) on Combustion, pp. 770-784, Academic Press, 1963.

7. Hall, J.G. and Russo, A.L., "Studies in Chemical Non-equilibrium in Hypersonic Nozzle Flows", Cornell Aero. Lab. Report No. AD-1118-A-6, 1959.

8. Reynolds, T.W. and Baldwin, L.V., "One Dimensional Flow with Chemical Reactions in Nozzle Expansion," Symposium on Thermodynamics of Jet and Rocket Propulsion, American Institute of Chemical Engineers, Kansas City, May 17-20, 1959.

9. Westenberg, A.A. and Favin, S., "Complex Chemical Kinetics in Supersonic Nozzle Flow": Ninth Symposium (International) on Combustion, pp. 785-798, Academic Press, 1963.

10. Sarli, V.J., Blackman, A.W., and Buswell, R.F., "Kinetics of Hydrogen-Air Flow Systems. II. Calculations of Nozzle Flows for Ramjets", Ninth Symposium (International) on Combustion, pp. 231-240, Academic Press, 1963.

11. Westenberg, A.A., "Hydrogen-Air Chemical Kinetic Calculations in Supersonic Flow", Applied Physics Laboratory, John Hopkins University, CM-1028, December 1962.

12. Sarli, V.J., "Investigation of Nonequilibrium Flow Effects in High Expansion Nozzles, Final Report", United Aircraft Corporation Report No. B910056-12, September 20, 1963.

PART III

EFFECT OF PASSAGE THROUGH A

SHOCK WAVE ON THE PROPERTIES

OF A REACTING GAS

By

Beverly J. Audeh

INTRODUCTION

The flow parameters of gases in a supersonic flow field are often computed by the method of characteristics, but this computation can not be extended across a shock wave. When a shock wave is encountered the characteristic net is usually allowed to approach the upstream side of the shock front and is then restarted on the downstream side of the shock, taking into account the change in properties across the shock.

When chemically reacting gas mixtures are involved, the evaluation of the properties along the restarting line can be quite important. A finite time is required for a mixture which has traversed a shock wave to reach its equilibrium condition. If the restarting line of the characteristic net is placed in such a location that equilibrium has not yet been attained, the actual values of the physical properties for the gas mixture at this point are between the frozen and equilibrium values. The calculation of the physical properties behind a shock using both a constant specific heat ratio case and an equilibrium case bracket the possible values that will be present on the non-characteristics restarting line.

LIST OF SYMBOLS

$[A_i]$	Mole fraction of A_i, dimensionless
c_p	Specific heat at constant pressure, cal/g°K
c_v	Specific heat at constant volume, cal/g°K
D	Dissociation energy, Kcal/mole
E_D	Energy from the dissociation process, cal/g
h	Enthalpy, cal/g
J	Mechanical equivalent of heat, ergs/cal
K.E.	Kinetic energy, cal/g
M	Molecular weight, g/g-mole
p	Pressure, atm
R	Gas constant, ergs/°K
s	Entropy, cal/g°K
T	Temperature, °K
u	Velocity, cm/sec
α'_{ij}, α''_{ij}	Stoichiometric coefficient of the i th species in the j th reaction, reactants and products respectively
β_{ij}	Number of atoms of the i th atomic species in the j th molecular species, atoms/molecule.
γ	Ratio of specific heats, c_p/c_v, dimensionless
ρ	Density, g/cm^3

Subscripts:

a	First value obtained in the iterative process
b	Second value obtained in the iterative process

i	Index
j	Index
1	Conditions ahead of the shock
2	Conditions behind the shock.

DISCUSSION

Methods of Calculation

Two cases bracket the possible physical properties behind the shock wave:

(1) the constant specific heat ratio case, and

(2) the case of equilibrium outside the shock region but including real gas effects caused by the shock.

The constant specific heat ratio case is solved using the Rankine-Hugoniot equations with the physical constants obtained from the initial conditions of the gas.

Calculation of equilibrium processes for a reacting gas requires a dual iteration to obtain physical properties of the gas which has passed through a shock wave. The first of the iterations is required to obtain the equilibrium partial pressures of the constituent gases at the assumed temperature behind the shock wave. These partial pressures are then used to obtain the energy of the gas and the new molecular weight of the mixture. The iteration upon the assumed temperature is checked by equating the energy made available by the shock as thermal energy to the energy used to raise the temperature and change the state of the gas. This procedure is given in detail in the Appendix and in Gaydon and Hurle (Ref. 1).

Availability of Computer Programs

Even for simple reactions the iterative solution is
long and detailed. For a system of reacting hydrogen and
oxygen in which at least eight reactions are considered of
importance at high temperatures and pressures (Refs. 2-4),
the evaluation of equilibrium properties for a given tempera-
ture requires the use of a digital computer. Two computer
programs were found to be available. The program described
in Ref. 5 will calculate equilibrium properties including
dissociated products. A program constructed at Marshall Space
Flight Center by Mr. Klaus Gross (Ref. 6) is patterned after
that of Ref. 5. The program developed by Zeleznik and Gordon
(Ref. 5) is presently being modified to include Debye-Huckel
effects and ionization potential lowering effects but these
will not be considered here. These effects are of little
importance except at high temperatures and low pressures.

The physical properties of hydrogen and oxygen required
by the general equilibrium programs are available in Refs.
5, 8, and 9. The above computer programs would require
certain modifications to enable read-out of the energy used
in the dissociation process. The dissociation energy is
required for the energy balance which determines the cor-
rect termination of the iteration. A program to handle the
entire iteration would essentially be an additional sub-
routine to either of the two equilibrium programs discussed
above.

Sample Computations

Hydrogen-Oxygen System. - To determine the applica-
bility of the computational procedures, one case for a
hydrogen-oxygen system was calculated. To enable the cal-
culation to be performed by hand, tables of thermodynamic
properties (Ref. 10) and tabulated values of dissociation
energies (Ref. 1) were used. This eliminated the first
iteration since equilibrium properties for given pressures
and temperatures were obtained by interpolation between the
values listed. The initial conditions applicable for both
cases considered; the conditions of the gas after it has
passed through a shock calculated for a constant specific
heat ratio case; and the properties of a gas with dissocia-
tion allowed in an equilibrium state after traversing a
normal shock are given in Table 1.

Table 1.

Properties of a Hydrogen-Oxygen System

Initial Conditions	Constant Specific Heat Ratio Case	Dissociating Equilibrium Case
$P_1 = 1$ atm	$P_2/P_1 = 98.81$	$P_2/P_1 = 104.33$
$T_1 = 700°K$	$T_2/T_1 = 14.98$	$T_2/T_1 = 6.429$
$h_1 = -2582.7$ cal/g	$T_2 = 10,490°K$	$T_2 = 4500°K$
$s_1 = 4.578$ cal/g°K	$\rho_2/\rho_1 = 6.594$	$\rho_2/\rho_1 = 13.035$
$M_1 = 10.08$	$\Delta s = 1.150$ cal/g°K	$\Delta s = 1.6627$ cal/g°K
$c_{P_1} = 0.7940$ cal/g°K	$c_{P_2} = 0.7940$ cal/g°K	$c_{P_2} = 5.698$ cal/g°K
$u_1 = 8.16 \times 10^5$ cm/sec		
$\gamma_1 = 1.3303$	$\gamma_2 = 1.3303$	$\gamma_2 = 1.1628$
		$[O_2] = 0.0077$
Mach No. = 9.309		$[O_1] = 0.0308$
$[H_1] = 0.0$	$[H_1] = 0.0$	$[H_1] = 0.2143$
$[H_2] = 0.4960$	$[H_2] = 0.4960$	$[H_2] = 0.3886$
$[H_2O] = 0.5040$	$[H_2O] = 0.5040$	$[H_2)] = 0.2565$
$[OH] = 0.0$	$[OH] = 0.0$	$[OH] = 0.1021$

Comparison of the results for the two cases indicates that the specific heat ratio decreases from 1.3303 for the frozen case to 1.1628 for the equilibrium calculation. The specific heat for the frozen flow assumption remained 0.7940

cal/g°K while in the equilibrium case it rose to 5.698 cal/g°K. This case was arbitrarily chosen to determine whether the computional procedure was correct. Since a hydrogen-oxygen mixture is highly active, the experimental data collected to date has been of experiments in which the reaction was repressed by addition of inert gases. The reactions taking place in the experiments are quite different from equilibrium processes of a pure mixture of these gases. A comparison of these computational results with actual experimental results has therefore not been made.

Carbon Dioxide System. - A sample calculation for CO_2 performed by Gaydon and Hurle (Ref. 1) listed values for both the constant specific heat ratio case and real dissociating gas in equilibrium case. The initial conditions of the gas; the conditions of the gas after it has passed through a normal shock calculated using a constant specific heat ratio; and the properties of the gas when treated as a real dissociating gas in equilibrium are presented in Table 2.

Table 2.

Properties of a Carbon Dioxide System

Initial Conditions	Constant Specific Heat Ratio Case	Dissociating Equilibrium Case
$p_1 = 1$ atm	$p_2/p_1 = 140$	$p_2/p_1 = 150$
$T_1 = 298°K$	$T_2/T_1 = 18.75$	$T_2/T_1 = 9.09$
$h_1 = 0$ cal/g	$T_2 = 5590°K$	$T_2 = 2710°K$
$M_1 = 44.01$	$M_2 = 44.01$	$M_2 = 39.40$
$u_1 = 3.0 \times 10^5$ cm/sec	$\rho_2/\rho_1 = 7.47$	$\rho_2/\rho_1 = 14.80$
Mach No. $= 11.15$		
$\gamma = 1.291$	$\gamma = 1.291$	$[O]_2 = 0.0092$
$[CO_2]_1 = 1.0000$	$[CO_2]_2 = 1.0000$	$[CO_2]_2 = 0.7172$
		$[CO]_2 = 0.1952$
		$[O_2]_2 = 0.0931$

Comparison of density ratios behind the shock obtained from theoretical and experimental evaluation of CO_2 are given in Ref. 11. Shock thickness was arbitrarily defined in Ref. 11 as the thickness required for the density ratio to become $\rho_2/\rho_1 = 6.0$. This comparison was shown for several levels of excitation of the vibrational modes. A reproduction of this comparison is shown in Fig. 1.

Placement of the Restarting Line

Vibration and dissociation relaxation times for CO_2 were found in Ref. 11 to be much longer than shock transit times. For a shock velocity of 3.0×10^5 cm/sec the vibration time was found to be 2.67 times that of the shock transit time and the dissociation time was 167 times longer. Assuming that the gas was traveling at a velocity corresponding to $u_2 = u_1/6$, the gas will travel 50 mean free paths behind the shock during the vibrational relaxation time and 3130 mean free paths during dissociation relaxation time. All mean free paths are calculated before the shock. For an original pressure of 0.015 torr these distances were calculated to be 7.5×10^{-4} mm and 4.5×10^{-2} mm respectively.

Since the processes within a shock wave and the relaxation regions behind it are quite complex, the placement of a characteristic restarting line sufficiently far downstream of the shock to insure that the gas would be in an equilibrium state would simplify the procedure. The distance required for the flow to reach its equilibrium values would appear to be negligibly small, i.e. 4.5×10^{-2} mm in the CO_2 example given above. Unless extremely rapid expansion immediately following the shock is encountered, the by-passing of this short distance will be unlikely to affect the final characteristic solution.

CONCLUSIONS

The chemical and physical properties of a gas computed for the cases of constant specific heat ratio through a normal shock and of the real gas in equilibrium after the shock, bracket the possible conditions at specific distances behind a normal shock. A comparison of the downstream properties obtained from the two cases for a hydrogen-oxygen system show large differences. Lack of experimental data for the H_2-O_2 system precludes comparison of the computations with test results. Available experimental data for a CO_2 system indicate that the gas travels only a short distance within the dissociation time after passing through a shock wave. The placement of a characteristic restarting line sufficiently far downstream of the shock to insure that the gas had reached its equilibrium condition can be used to simplify the computation procedure. Unless extremely rapid expansion immediately following the shock exists, the use of equilibrium properties along the restarting line should not adversely affect the final characteristic solution.

REFERENCES

1. Gaydon, A.G. and Hurle, I.R., The Shock Tube in High Temperature Chemical Physics, Reinhold Publ. Corp., New York, 1963.

2. Ferri, A., "Review of Problems in Application of Supersonic Combustion", Journal of Royal Aeronautical Society,

Vol. 68, No. 645, September 1964.

3. Westenberg, A.A., "Hydrogen - Air Chemical Kinetic Calculations in Supersonic Flow", Applied Physics Lab., CM-1028, December 1962.

4. Ferri, A., Moretti, G., and Slutsky, S., "Mixing Processes in Supersonic Combustion", Society for Industrial and Applied Mathematics National Meeting, Washington, D.C., May 11-14, 1964.

5. Zeleznik, F.J. and Gordon, S., "A General IBM 704 or 7090 Computer program for Computation of Chemical Equilibrium Compositions, Rocket Performance, and Chapman--Jouguet Detonations", NASA TN D-1454, October 1962.

6. Gross, Klaus, "Computer Program to Determine Equilibrium Composition", P. & V.E., MSFC (to be Published).

7. Gordon, S., Private Communication, January 1965.

8. McGride, B.J., Heimel, S., Ehlers, J.G., and Gordon, S., "Thermodynamic Properties to 6000°K for 210 Substances Involving the First 18 Elements", NASA SP-3001, 1963.

9. Stull, D.R., "JANAF Interim Thermochemical Tables", Dow Chemical Co., Midland Michigan, March 1964.

10. Svehla, R.A., "Thermodynamic and Transport Properties for the Hydrogen-Oxygen System", NASA SP-3011, 1964.

11. Camac, Morton, "CO_2 Relaxation Processes in Shock Waves", AVCO Research Report 194, October 1964.

APPENDIX

CALCULATION OF THE EQUILIBRIUM STATE
OF A REAL DISSOCIATING GAS

Given: p_1, T_1, u_1, and gas composition at position 1.

Determine: p_2, T_2, ρ_2/ρ_1 and final gas composition at position 2.

Assume: The gas exhibits the properties of a real gas at equilibrium at positions 1 and 2.

Calculation Procedure:

(i)   Assume a value for T_2 and p_2

(ii)   Determine the partial pressure or mole fraction and the molecular weight M_2 of the shocked gas using the assumed T_2 and p_2 in the following equations:

$$\sum \alpha'_{ij} A_i \; \underset{\rightarrow}{\overset{\leftarrow}{\;}} \; \sum \alpha''_{ij} A_i \tag{1}$$

$$Keq_j = \prod_{i=1}^{n} \frac{[A_i]^{\alpha''_{ij}}}{[A_i]^{\alpha'_{ij}}} \tag{2}$$

$$\sum_{i=1}^{n} [A_i] = p_2 \tag{3}$$

$$M_2 = \frac{1}{P_2} \sum (M_1[A_i]) \qquad (4)$$

$$\frac{\text{Number of Atoms of Element } i}{\text{Number of Atoms of Element } j} = \frac{\sigma_i}{\sigma_j} \times \frac{\sum\limits_{j} \beta_{ij}[A_j]}{\sum\limits_{i} \beta_{ji}[A_i]}. \qquad (5)$$

(iii) Use the partial pressures, $[A_i]$'s, and the value of M_2 to obtain the value of h_2 and ΔE_D from

$$h_2 = \frac{1}{M_2 P_2} \sum [A_i] h_{A_i} \qquad (6)$$

$$\Delta E_D = \sum \alpha_{ij} \frac{[A_i]_{diss}}{P_2 M_2} D_{A_i} \text{ undiss.} \qquad (7)$$

(iv) Calculate ρ_2/ρ_1 from the following equation using the assumed T_2 and p_2 with M_2:

$$\frac{\rho_2}{\rho_1} = \left(\frac{p_2}{p_1}\right)\left(\frac{T_1}{T_2}\right)\left(\frac{M_2}{M_1}\right) . \qquad (8)$$

(v) Evaluate kinetic energy from

$$K.E. = 1/2 \frac{u_1^2}{J} \left[1 - \left(\frac{\rho_1}{\rho_2}\right)^2\right] \qquad (9)$$

(vi) Use the h_2 from step (iii) to calculate $(h_2 - h_1)_a$

(vii) Compare the value from step (vi) with that obtained

by

$$(h_2 - h_1)_b = (K.E.)_b - \Delta E_D \qquad (10)$$

If $|(h_2 - h_1)_a - (h_2 - h_1)_b| < \epsilon$, an arbitrary maximum allowable error, the iteration is complete. Otherwise, another choice of T_2 is required and the iteration repeated.

(viii) When the balance of energies is obtained, use the ρ_2/ρ_1 ratio from step (iv) to evaluate a final p_2/p_1 from

$$\frac{p_2}{p_1} = 1 + \frac{M_1 u_1^2}{R T_1} \left(1 - \frac{\rho_1}{\rho_2} \right) \qquad (11)$$

(ix) Use this p_2/p_1 value with the final T_2 value to obtain the final ρ_2/ρ_1 from the following equation:

$$\frac{\rho_2}{\rho_1} = \left(\frac{p_2}{p_1} \right) \left(\frac{T_1}{T_2} \right) \left(\frac{M_2}{M_1} \right) \qquad (8)$$

(x) With the final T_2, p_2/p_1, and ρ_2/ρ_1, determine the equilibrium composition of gas at station (2) using step (ii).
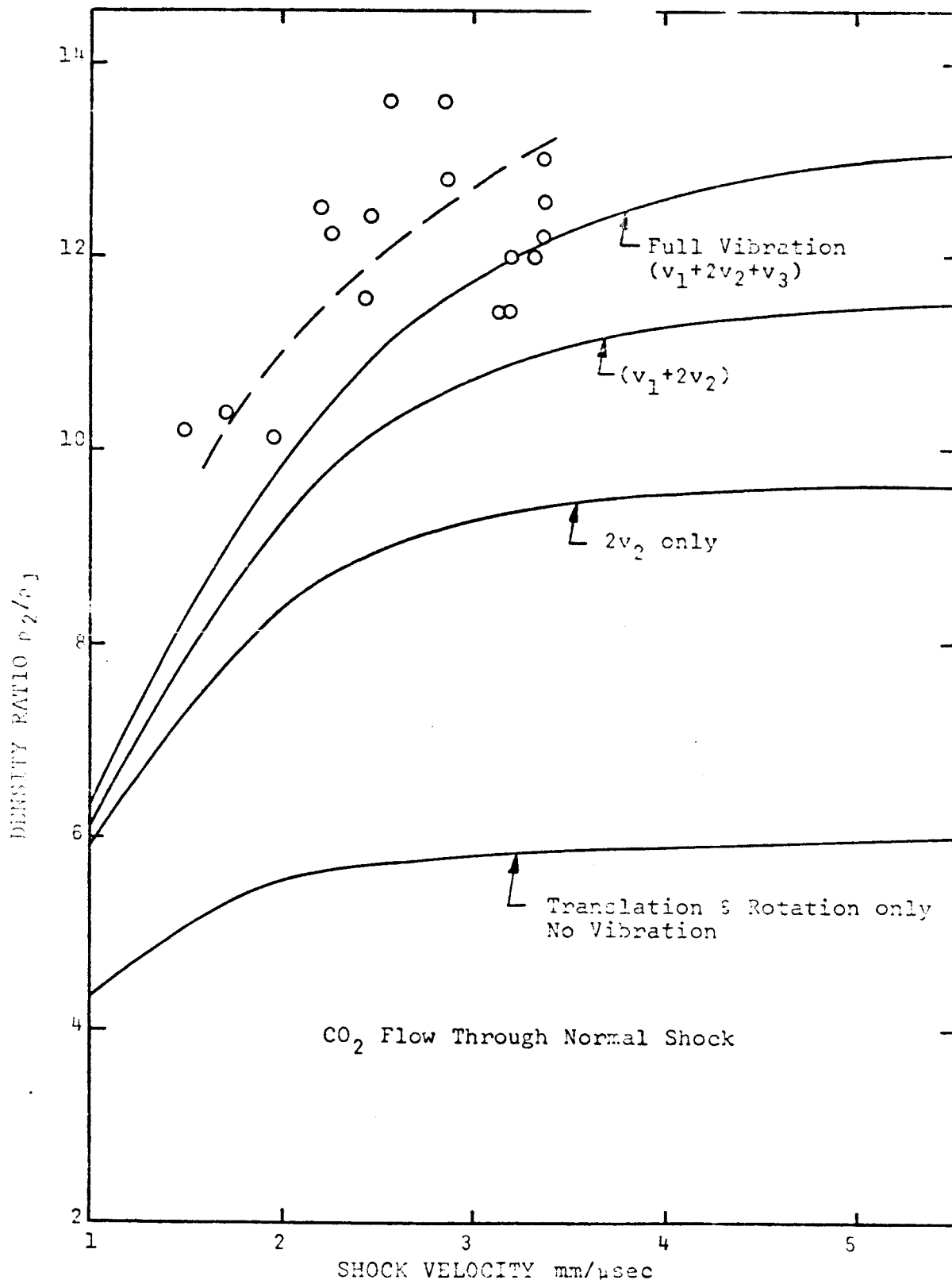
Fig. 1 Solid curves show the calculated density ratio across shock
for various assumptions on the excitation of vibration modes.
The points are experimental measurements. The dashed line is
through the center of the experimental data.

PART IV

SPECIFIC HEAT VARIATION THROUGH

A NORMAL SHOCK

By

Beverly J. Audeh

INTRODUCTION

The passage of a shock wave through a gas causes a rapid change in the gas properties such as temperature and pressure. The various energy modes that define the temperature of the gas, however, do not adjust instantaneously, or at the same rate, to the new conditions following the passage of the shock. Scala and Talbot (Refs. 1 and 2) investigated the relaxation of these energy modes and chose a relaxation model with direct coupling between rotational and vibrational temperatures and an indirect coupling through the translational temperature. This model was used to calculate temperature profiles through a normal shock. A method is presented in this study to use these temperature profiles to determine the variation of specific heats of a non-reacting gas through a normal shock wave.

LIST OF SYMBOLS

B_e Rotational spectroscopic constant

B_v Spectroscopic constant, defined by Eq. 17

c Speed of light, cm/sec

$\bar{c}$ Mean molecular speed, cm/sec

C_p Specific heat at constant pressure, cal/g°K

D_e Rotational stretching constant

D_v Spectroscopic constant, defined by Eq. 18

E_i Energy of i th state, cal/g

e Electronic state

g_i Quantum mechanical degeneracy of i th energy state

h Planck's constant, erg/sec

J Rotational quantum number for molecules

k Boltzmann constant, erg/°K

L Mean free path, cm

m Mass, g

Q Partition function

r_e Internuclear distance, cm

s Entropy, cal/g°K

s' Symmetry factor

T Temperature, °K

v Vibrational state

V Volume, cm^3

x_j Mole fraction of the j th component

x_e Vibrational spectroscopic constant, cm^{-1}

y_e Vibrational spectroscopic constant, cm^{-1}

z_e Vibrational spectroscopic constant, cm^{-1}

α_e Rotational-vibrational coupling constant

β Relaxation time, sec

β_e Rotational-vibrational coupling constant

η Viscosity, g/cm sec

μ Reduced mass of molecule

ψ_i Average number of intermolecular collisions required for relaxation

ω_e Vibrational spectroscopic constant, cm^{-1}

Subscripts:

e   Dependence upon the electronic state

i   Energy state index

int   Internal energy state

j   Species index

r   Dependence upon the rotational state

trans   Translational energy states

DISCUSSION

Partition Functions

The required partition functions are briefly described here in a fashion similar to that given by Drellishak (Ref. 3). The partition function for a single particle is defined as

$$Q = \sum_i g_i \, e^{\frac{-E_i}{kT}} \qquad (1)$$

where the summation is made over all allowable energy levels, E_i. The energy levels, E_i, can be written in more detail as

$$E_i = E_{trans} + E_e + E_v(e) + E_r(v,e) \qquad (2)$$

where: E_{trans} = translational energy of the particle

E_e = electronic excitation energy

$E_v(e)$ = vibrational energy of a molecular constituent

$E_r(v,e)$ = rotational energy.

If the last three terms in Eq. 2 are called internal energy modes, the energy of the particle can be written in the following form:

$$E_i = E_{trans} + E_{int} \cdot \qquad (3)$$

Because of the mathematical form of Eq. 2 and 3, the partition function can be rewritten as

$$Q = Q_{trans} \, Q_{int} \, .$$ (4)

The sum over all translational energy states, Q_{trans}, can be evaluated as

$$Q_{trans} = (2\pi mkT/h^2)^{3/2} \, V$$ (5)

and over all internal energy states, Q_{int}, as

$$Q_{int} = \sum_e \left\{ g_e \, e^{-\frac{E_e}{kT}} \left[\sum_v g_v \, e^{-\frac{E_v(e)}{kT}} \left(\sum_r g_r \, e^{-\frac{E_{r(e,v)}}{kT}} \right) \right] \right\}$$ (6)

where the summations over e, v, and r mean that the summations are to be taken respectively over all allowable electronic, vibrational, and rotational energy states of the particle.

Rigid Rotator-Harmonic Oscillator. - For cases in which the temperature levels are limited, the simple representation by a model of a rigid rotator-harmonic oscillator gives much useful information. For this model the vibrational energy can be written in the following form:

$$E_v = hc\omega_e \, (v + 1/2).$$ (7)

If the energy is referenced to the zero point vibrational energy, $E_o(e)$, Eq. 7 can be rewritten as

$$\frac{E_v(e) - E_o(e)}{hc} = \omega_e v \qquad (8)$$

where: $\omega_e = \dfrac{v_{osc}}{c}$.

The equation for the allowable rotational energy states may be written as

$$\frac{E_r}{hc} = B_e \, J \, (J + 1) \qquad (9)$$

where:

$$B_e = \frac{h}{8\pi c \mu r_e^2} \qquad (10)$$

Eq. 10 represents indirectly the moment of inertia of the rotator.

The symbol J in Eq. 9 is the rotational quantum number which can take on all integer values. In the definition of B_e, the value of the reduced mass, μ, of the molecule is defined as

$$\mu = \frac{m_1 m_2}{m_1 + m_2} .$$

The degeneracy corresponding to the rotational mode is

$$g_r = 2J + 1. \qquad (11)$$

Using the reference level as the zero point vibration energy and with $g_v = 1$ for all v, the vibrational partition function is written as

$$Q_v = \sum_{v=0}^{\infty} e^{-\left(\frac{hc\omega_e v}{kT}\right)}. \qquad (12)$$

Eq. 12 may be rewritten as

$$Q_v = \left[1 - e^{-\left(\frac{hc\omega_e}{kT}\right)}\right]^{-1}. \qquad (13)$$

Using Eq. 9 and 11, the rotational contribution to the internal partition function becomes

$$Q_r = \frac{1}{s'} \sum_{J=0}^{\infty} (2J + 1)e^{-\left(\frac{hcB_e J(J + 1)}{kT}\right)}. \qquad (14)$$

In Eq. 14, s' is a symmetry factor which is two for symmetrical diatomic molecules and one for unsymmetrical diatomic molecules.

Coupled Vibration and Rotation. - When temperatures higher than the limits of applicability of the rigid rotator-harmonic oscillator occur, the effect of coupling between the vibration and rotation modes must be included. In this case a semi-empirical expression is needed to represent the vibrational energy accurately. The following equation is formulated for that purpose:

$$\frac{E_v(e)}{hc} = \omega_e(v + 1/2) - \omega_e x_e (v + 1/2)^2 +$$

$$\omega_e y_e(V + 1/2)^3 + \omega_e z_e(v + 1/2)^4 + \ldots \quad (15)$$

where $\omega_e x_e$, ... are spectroscopic constants.

Because of coupling, the rotational energy is now written as

$$\frac{E_r(e,v)}{hc} = B_v J(J + 1) - D_v J^2(J + 1)^2 \quad (16)$$

where: $B_v = B_e - \alpha_e (v + 1/2)$ \quad (17)

$$D_v = D_e - \beta_e (v + 1/2) \quad (18)$$

$$D_e = \frac{4 B_e^3}{\omega_e^2} \quad . \quad (19)$$

The last term, $D_v J^2(J + 1)^2$, accounts for the centrifugal

stretching effect which may be considered as the potential energy of rotation.

Just as placing limits upon the temperature considered could make the rigid rotator-harmonic oscillator applicable, the temperature limits can be set such that ionization effects are of negligible importance. This limitation eliminates the evaluation of the partition function for electronic excitation. In this restricted case, the partition function can be described by the translational, vibrational, and rotational modes.

Evaluation of the The Thermodynamic Properties

To obtain the thermodynamic properties the partition functions calculated are used in a systematic method. The entropy may be evaluated from the following equation:

$$s_i = k \log Q_i + k T_i \left(\frac{\partial Q_i}{\partial T_i} \right)_p . \tag{20}$$

Using these values of entropy in

$$C_{p_i} = T_i \left(\frac{\partial s_i}{\partial T_i} \right)_p \tag{21}$$

the contribution from the various energy levels to the specific heat is obtained. The specific heat for species j is the sum of all the components.

$$C_{p_j} = \sum_i C_{p_i} \tag{22}$$

For non-reacting gas mixtures (Ref. 4)

$$C_{P_{mix}} = \sum_j x_j \, C_{P_j} \qquad (23)$$

where x_j is the mole fraction of the j th component.

Introduction of Nonequilibrium Effects Into
Equilibrium Partition Function Equations

Application of these partition functions and thermo-
dynamic equations through a shock is dependent upon several
assumptions or restrictions. The most rigid restriction is
the necessity that these equations be used for equilibrium
conditions. The assumption that the temperature variation
through the shock occurs in a stepwise manner can be used
to satisfy this requirement. Though the temperatures of
the various modes are not necessarily equal, the modes are
assumed to be in equilibrium at their respective temperatures.
For example, this implies that the partition function for the
rotational mode can be written with the rotational temperature,
T_r, as if the equilibrium temperature were this rotational
temperature. Since the temperature profiles were defined
in such a manner that they indicate the deviation from equili-
brium, the use of these component temperatures (T_r, T_v, and T_t)
in the partition functions provides a method to introduce
non-equilibrium effects and still allow application of equilibrium

equations. After the individual partition functions are evaluated, the differing species are treated as ideal gases and combined as a mixture of ideal gases.

Temperature Profiles

A mathematical model of the temperature in which there is direct coupling between T_r and T_v, and indirect coupling through T_t was developed by Talbot and Scala (Ref. 2). The shock wave strengths were arbitrarily picked. The number of intermolecular collisions required to reach a state of equilibrium is not yet well established. The temperature profiles mentioned above are determined for parametric values of the molecular collisions required for equilibrium to be attained. A relaxation time, β_i, may be related to the average number, ψ_i, of intermolecular collisions. The mean molecular speed, $\bar{c}$, and the mean free path, $\bar{L}$, are also involved with this relation in the following manner:

$$\beta_i = \frac{\psi_i \bar{L}}{\bar{c}} = \frac{\pi \, \psi_i \, \eta}{4 \, p} . \tag{24}$$

Experimental values for relaxation times are limited in quantity. Some values for relaxation times are given for shock waves in CO_2 in Ref. 5 and for N_2 in Ref. 6.

Use of the above equations allows an approximate determination of the value of ψ_i corresponding to the experimentally

determined relaxation time, β_i. Using these ψ_i values, a calculation of the temperature relaxation profiles using the model outlined by Talbot and Scala will provide a check upon the accuracy of the model itself. If there is sufficient accuracy of the model, available experimental values of relaxation time would provide temperature profiles through other shock waves.

RECOMMENDATIONS

1. Experimental values for temperature profiles and relaxation times are available for normal shock waves in CO_2. It is recommended that these relaxation times be used to calculate temperature profiles using the mathematical model with both direct and indirect coupling of the temperatures.

2. If the mathematical model is then determined to be sufficiently correct, relaxation times can be used to evaluate temperature profiles throughout other shock waves.

3. It is recommended that the use of equilibrium partition functions to determine specific heat variation through a shock should be extended to include reacting and ionizing gases.

REFERENCES

1. Talbot, L. and Scala, S.M., "Shock Wave Structure in a Relaxing Diatomic Gas," Rarefied Gas Dynamics, Talbot, L., ed., Vol. 1, Academic Press, New York (1961).

2. Scala, S.M. and Talbot, L., "Shock Wave Structure with Rotational and Vibrational Relaxation", Rarefied Gas Dynamics, Laurmann, J.A., ed., Vol. 1, Academic Press, New York (1963).

3. Drellishak, K.S., "Partition Functions and Thermodynamic Properties of High Temperature Gases", AEDC-TDR-64-22, January 1964.

4. Hirschfelder, J.O., Curtiss, C.F., and Bird, R.B., Molecular Theory of Gases and Liquids, Wiley Press, New York, 1954.

5. Camac, M., "CO_2 Relaxation Processes in Shock Waves", AVCO Research Report 194, October 1964.

6. Allen, R.A., "Nonequilibrium Shock Front Rotational, Vibrational and Electronic Temperature Measurements", AVCO Research Report 186, August 1964.

PART V

THE APPLICABILITY OF LATVALA'S METHOD

OF CIRCULAR ARCS FOR PREDICTING

SATURN PLUME BOUNDARIES

By

L. H. Usher

INTRODUCTION

The exhaust jet of a rocket engine expands until the jet boundary pressure is equal to the ambient pressure. With operation at high altitudes, adjacent rocket engine exhaust plumes may impinge mutually and interact with the free stream, thus resulting in reverse flow of hot gases and in other phenomena associated with base heating of vehicles. It is desirable, therefore, to be able to predict changes in the plume boundaries due to change in altitude.

There are several methods of approximating the shape of the exhaust plumes which do not require the use of lengthy computations. The method of circular arcs as presented by Latvala (Ref. 1) is an empirical method of approximating the initial shape of the plume boundary. Using this technique, useful approximations of the plume shape near the nozzle exit may be calculated very readily for expansion of a single supersonic jet into quiescent air, but mutual jet interaction for clustered engine configurations and flight aerodynamic interference effects are not considered. It is the purpose of this investigation to determine whether Latvala's method may be applied to prediction of flight plume boundaries for such vehicles as the SATURN.

DISCUSSION

Comparisons were made between plume boundaries pre-
dicted by Latvala's method and visible plume boundaries shown
in photographs of the SATURN SA-1 flight. Photographs of the
SATURN SA-1 flight were obtained for the portion of vehicle
trajectory between 11.71 Km and 49.22 Km. The luminous out-
line of the plume boundary was visible in these photographs
and was traced as shown in Fig. 1a thru Fig. 1L. This luminous
outline is assumed to approximate the true plume boundary.

The plume boundaries as observed in these photographs
are slightly distorted due to the changing attitude of the
vehicle with respect to the point of observation. Over the
altitude range under observation, however, this distortion
is considered negligible. Other effects which might create
some error are the vehicle angle-of-attack and engine tilt.
These effects, also, are considered negligible.

The pressure altitude corresponding to each of the
photographs was taken from Ref. 2. A Prandtl-Meyer expan-
sion from the nozzle lip to this pressure altitude was used
to calculate the inclination of the circular arc plume boundary
at the nozzle exit. The expansion was made from the 165K
thrust H-1 engine using the following equation,

$$\alpha_1 = \nu_1 - \nu_j + \theta_n$$

where:

α_1 = The inclination of the plume boundary at the nozzle exit

v_1 = Prandtl-Meyer turning angle corresponding to the pressure altitude to combustion chamber pressure ratio, (P_c = 578 psia)

v_j = Prandtl-Meyer turning angle corresponding to the nozzle exit Mach number, (M_{exit} = 3.12)

θ_n = The nozzle exit cone angle (= 9.25°).

The circular arc radius of the plume was obtained from Ref. 1 which gives an experimentally determined curve of (R/r_j) versus the nozzle exit Mach Number for the case of γ = 1.4. Then the following equation (Equation (2) of Ref. 1),

$$(R/r_j) = (R/r_j)_{1.4} \frac{(\gamma + 1)(5 + M_j^2)}{12 \left[1 + \frac{\gamma-1}{2} M_j^2\right]}$$

where:

R = Radius of circular arc

r_j = Radius of jet exit

M_j = Mach number at jet exit

γ = Specific heat ratio

was used to correct the radius ratio $(R/r_j)_{1.4}$ to the proper specific heat ratio. A specific heat ratio (γ) of 1.14, which is characteristic of the engine under consideration, was used in these calculations.

Circular arc approximations of the plume boundaries
are shown in the figures for comparison with boundaries ob-
tained from the photographs. At altitudes between 11.71 Km
and 24.86 Km the approximations fit the flight plume boundaries
quite well as shown in Fig. 1a thru Fig. 1d. At higher
altitudes, however, during the period of high free stream
dynamic pressure with the resulting aerodynamic interference
effects, the approximation does not compare favorably with the
photographs (Fig. 1e thru 1j). Favorable comparisons appear
to again be achieved at the extremely high altitudes of Figs.
1k and 1L. At this altitude, the free stream dynamic pressure
is once again very small and there is little aerodynamic
interference.

CONCLUSIONS

Latvala's method of circular arcs appears to be useful
for the prediction of plume boundaries for the SATURN I
clustered engine configuration under flight conditions at
which free stream aerodynamic interference effects are not
severe. For the trajectory of SATURN flight SA-1 the method
gave good results over an altitude range up to about 25 Km
and above about 50 Km.

REFERENCES

1. Latvala, E.K., "Spreading of Rocket Exhaust Jets at High Altitudes", AEDC-TR-59-11, June 1959.

2. Smith, O.E., "A Reference Atmosphere for Patrick AFB, Florida", NASA TN D-595, March 1961.

$\alpha_1 = 53.35°$

Circular Arc
Approximation
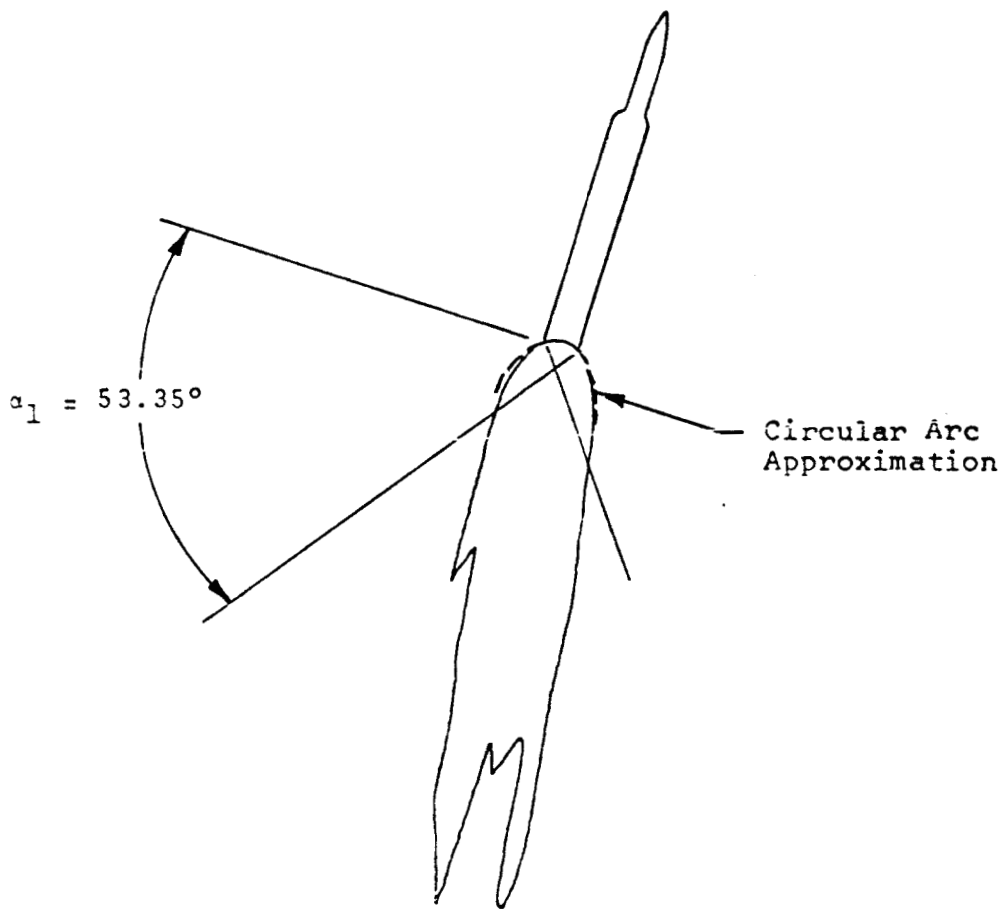
FIG. 1a   COMPARISON OF JET BOUNDARIES CALCULATED
BY THE METHOD OF CIRCULAR ARCS WITH
SATURN SA-1 PHOTOGRAPHS

$\alpha_1 = 56.35°$

FIG. 1b

Flight Conditions
Time = 79.08 sec
Alt. = 20.69 KM
M. = 2.44
SA-1

$\alpha_1 = 61.35°$

FIG. 1c

-56-
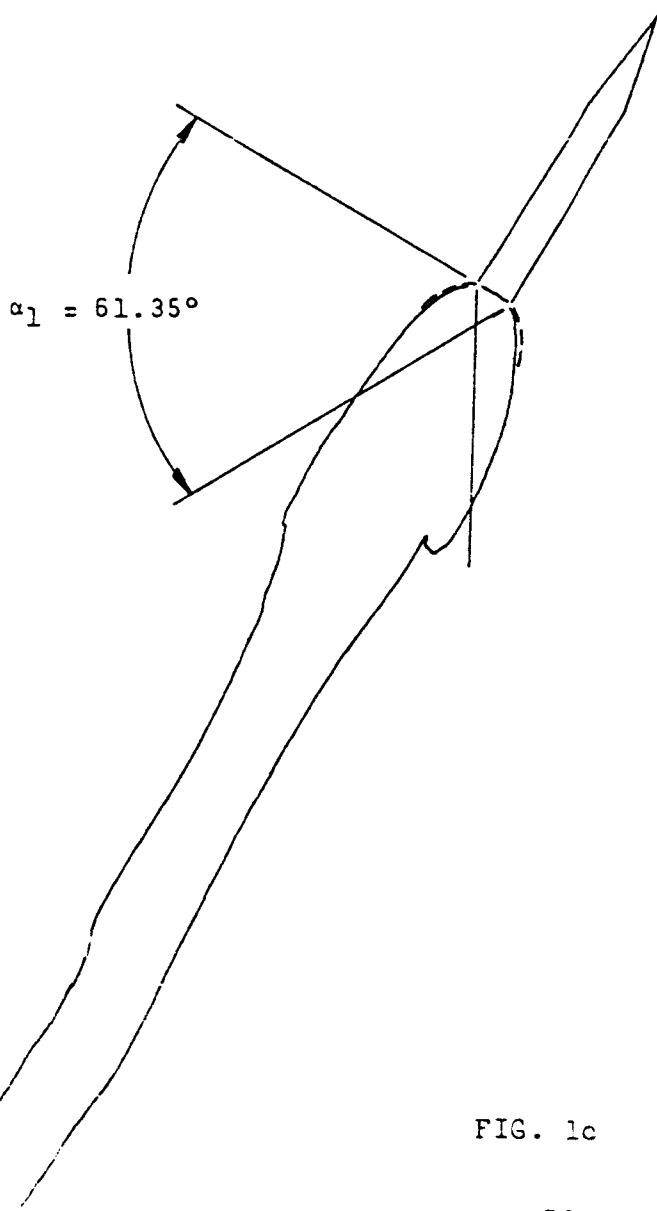
Flight Conditions
Time = 85.08 sec
Alt. = 24.86 KM
M. = 2.80
SA-1
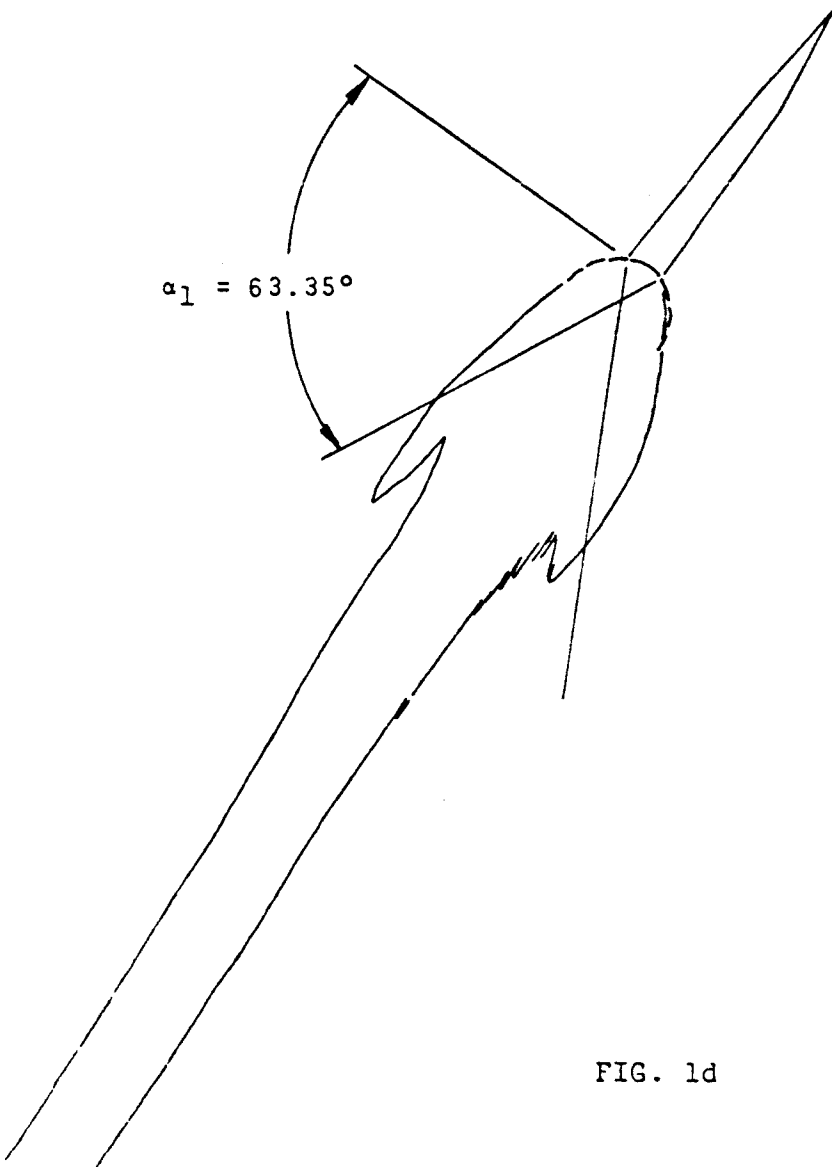
$\alpha_1 = 63.35°$

FIG. 1d

$\alpha_1 = 66.35°$

FIG. 1e

$\alpha_1 = 68.35°$
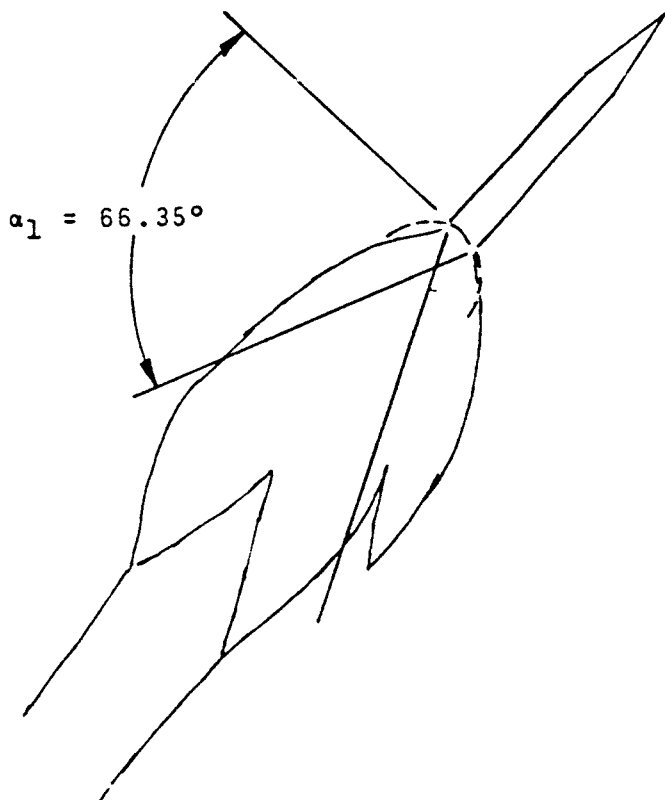
FIG. 1f

Flight Conditions
Time = 98.08 sec
Alt. = 35.80 KM
M = 3.65
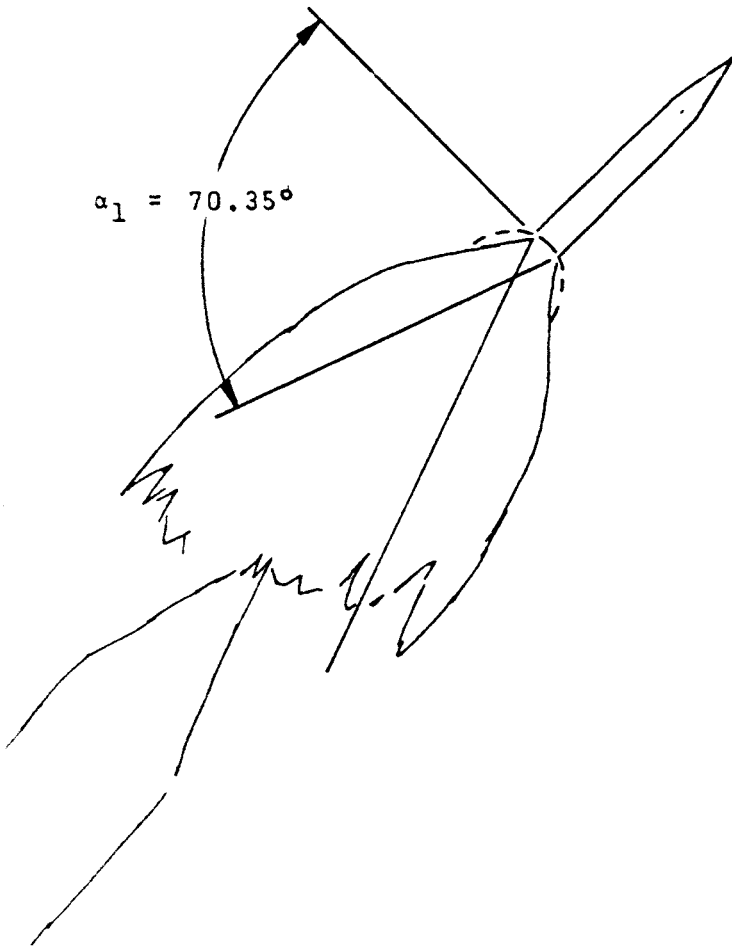SA-1

$\alpha_1 = 70.35°$

FIG. 1g

Flight Conditions
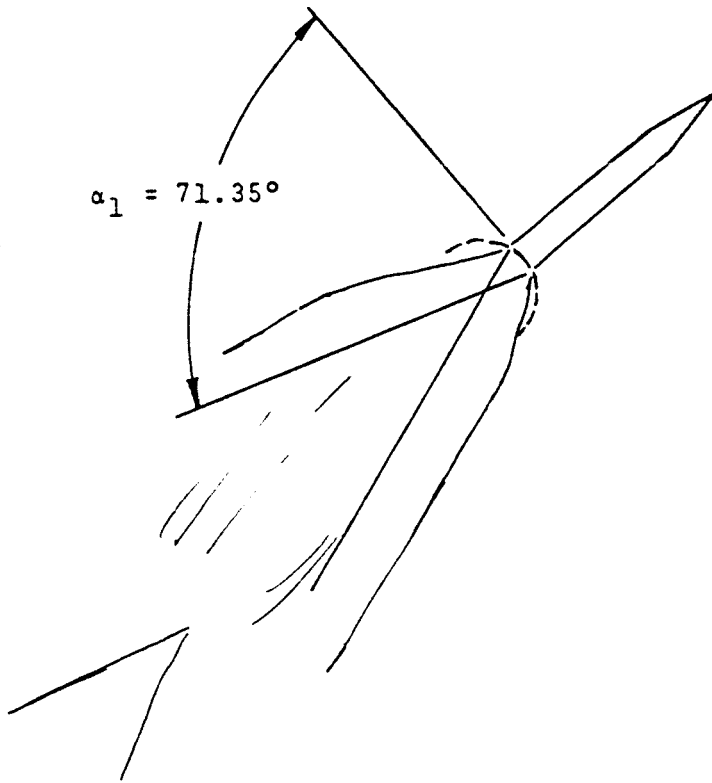Time = 100.08 sec
Alt. = 37.73 KM
M = 3.79
SA-1

$\alpha_1 = 71.35°$

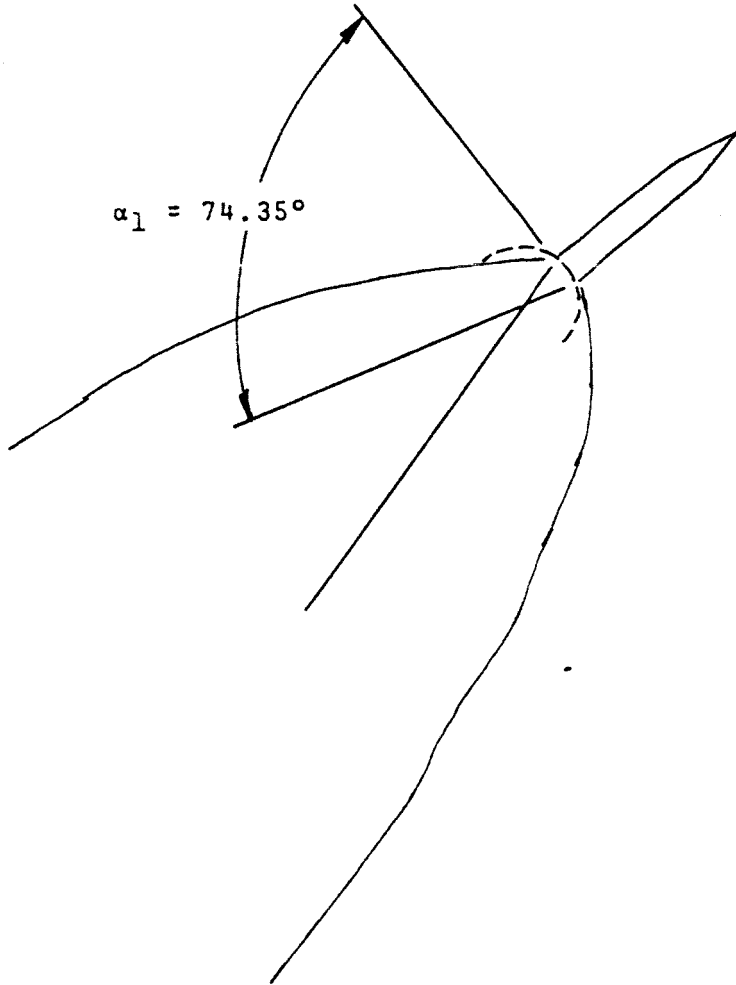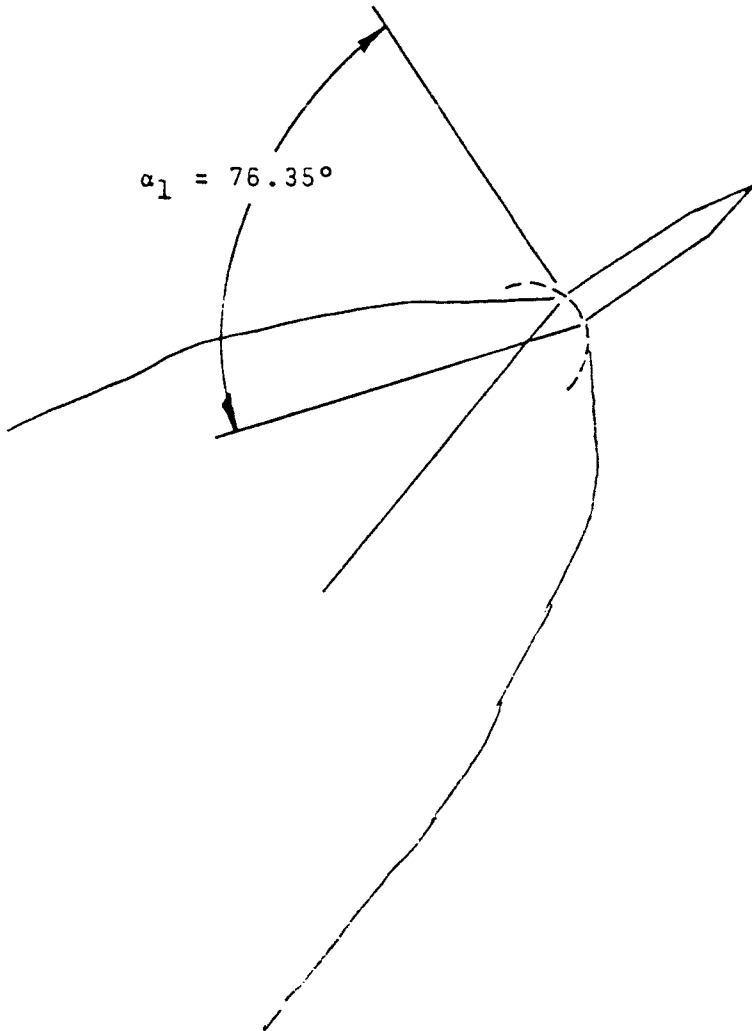FIG. 1h

Flight Conditions
Time = 104.58 sec
Alt. = 42.32 KM
M = 4.12
SA-1

$\alpha_1 = 74.35°$

FIG. 1i

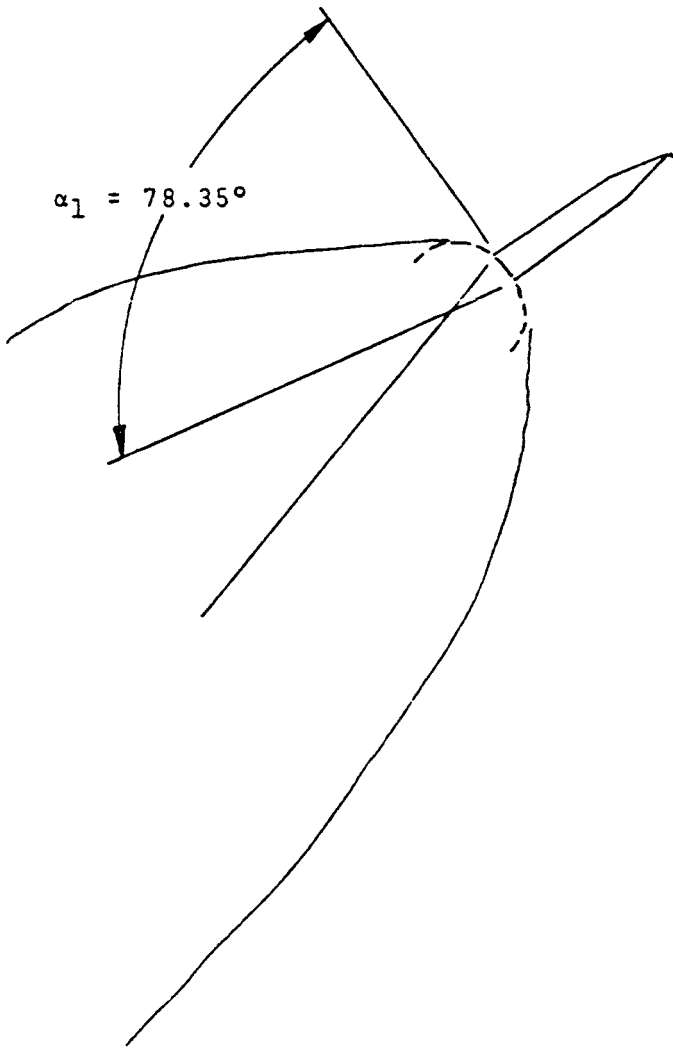$\alpha_1 = 76.35°$

$\alpha_1 = 78.35°$

FIG. 1k

Flight Conditions
Time = 110.73 sec
Alt. = 49.22 KM
M.. = 4.56
SA-1

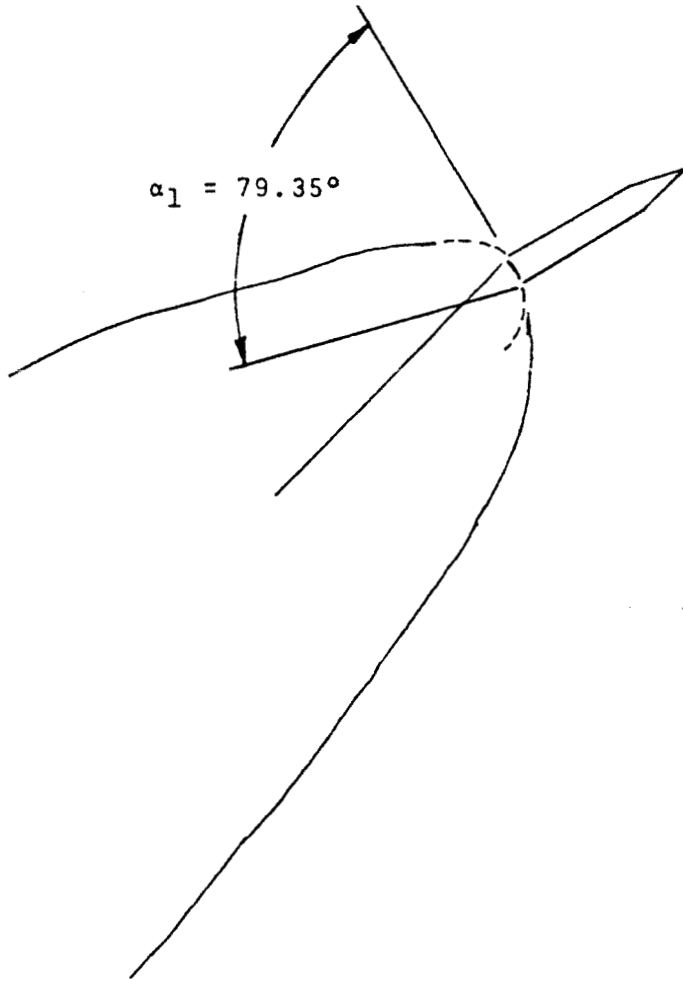$\alpha_1 = 79.35°$

FIG. 1L

PART VI

DETERMINATION OF VELOCITIES

IN A TURBULENT GAS STREAM

FROM SCATTERING OF A

MONOCHROMATIC LIGHT BEAM

By

S. J. Robertson

A. Datis

and

H. Y. Yen

INTRODUCTION

Marshall Space Flight Center (MSFC) is sponsoring the development of an optical technique for velocity measurements in gas flow. This technique is based on determination of velocity from measurements of the Doppler shift of a monochromatic light beam scattered from moving particles suspended in the gas stream. The monochromatic light source used in these measurements is a continuous beam helium-neon gas laser with vacuum beam wavelength of $6328\overset{\circ}{A}$. The particle suspension is produced by injecting smoke in the gas stream.

This method was applied by the developing contractor to the measurement of velocities in a turbulent gas stream flowing through a 1" x 3" rectangular test section. Due to the turbulent velocity fluctuations, the measured Doppler shift frequency of the scattered light beams varied over a spectrum corresponding to the varying velocities in the fluctuating flow.

Heat Technology Laboratory has developed the theoretical technique for reduction of the data and performed an analysis of the measured Doppler shift frequencies to determine the relationship between the Doppler shift frequency spectrum and the velocity fluctuations in the gas stream.

THEORY

The analysis of the Doppler shift frequency spectrum is treated below in a manner similar to the treatment of the Doppler broadening of line spectra.

The Doppler shift frequency, f_D, in cycles per unit time of a monochromatic light beam scattered from a moving particle is given by:

$$f_D = (\vec{k} - \vec{k_o}) \cdot \vec{V} \tag{1}$$

where $\vec{k}$ is the wave vector of the scattered beam, $\vec{k_o}$ is the wave vector of the incident beam, and $\vec{V}$ is the velocity vector of the particle.

The vectors $\vec{k}$ and $\vec{k_o}$ have their directions in the direction of propagation and absolute values:

$$|k| = \frac{1}{\lambda} \quad \text{and} \quad |k_o| = \frac{1}{\lambda_o} \tag{2}$$

where λ is the wavelength of the scattered beam and λ_o is the wavelength of the incident beam. λ is assumed in this analysis to be equal to λ_o.

The instantaneous velocity vector $\vec{V}$ of a single moving particle in the gas stream may be represented by:

$$\vec{V} = \vec{\bar{V}} + \vec{v} \tag{3}$$

where $\overline{\underset{\rightarrow}{V}}$ is the mean flow velocity vector of the gas stream

and $\underset{\rightarrow}{v}$ is the superimposed turbulence velocity vector.

For purposes of this analysis, the fluctuating velocity $\underset{\rightarrow}{v}$ will be assumed to be completely isotropic, with a Gaussian probability distribution of velocities given as follows:

$$f\,(v_x) = \frac{\beta}{\sqrt{\pi}} \, \exp \, (-\beta^2 v_x{}^2)$$

$$f\,(v_y) = \frac{\beta}{\sqrt{\pi}} \, \exp \, (-\beta^2 v_y{}^2) \qquad (4)$$

$$f\,(v_z) = \frac{\beta}{\sqrt{\pi}} \, \exp \, (-\beta^2 v_z{}^2)$$

in analogy with the kinetic theory of gases. The parameter β is a measure of the "width" of the turbulence velocity distribution curve and is related to the root-mean-square of a turbulence velocity component as follows:

$$\sqrt{\overline{v_x{}^2}} = \left\{ \int_{-\infty}^{\infty} v_x{}^2 \, f(v_x) \, dv_x \right\}^{1/2} = \frac{1}{\sqrt{2}\,\beta} \qquad (5)$$

The intensity of turbulence, T, is usually defined for isotropic turbulence as the ratio of the root-mean-square of a turbulence velocity component to the magnitude of the mean flow velocity vector:

$$T = \frac{\sqrt{\overline{v_x^2}}}{\overline{V}} = \frac{1}{\sqrt{2} \; \beta \; \overline{V}} \tag{6}$$

The experimental setup for measuring the Doppler shift frequency spectrum is shown schematically as follows:
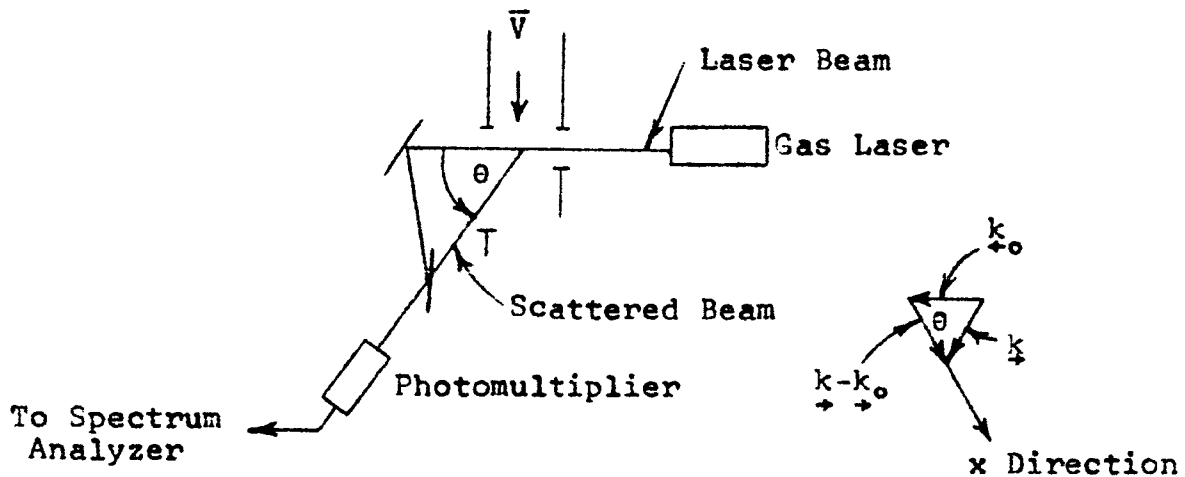
The Doppler shift frequency from Eq. 1 is given as follows for a rectangular coordinate system with the x direction in the direction of $(\vec{k} - \vec{k_o})$

$$f_D = (\vec{k} - \vec{k_o}) \cdot \vec{V} = \frac{1}{\lambda_o} (\overline{V} \sin \theta + 2 \, v_x \sin \frac{\theta}{2}) \tag{7}$$

Scattering from particles with velocities with components in the range dv_x will result in Doppler shift frequencies in the range df_D as follows:

$$df_D = \frac{2 \sin \frac{\theta}{2}}{\lambda_o} \, d \, v_x \tag{8}$$

The number of scattered beams in the frequency range df_D will be proportional to the number of particles with velocity components in the range dv_x:

$$J \, df_D = J \, \frac{2 \sin \frac{\theta}{2}}{\lambda_0} \, dv_x = K \, \frac{\beta}{\sqrt{\pi}} \, e^{-\beta^2 v_x^2} \, dv_x \tag{9}$$

where J represents the spectral intensity of the scattered radiation and K is a proportionality constant.

Substituting the expression for v_x obtained from Eq. 7 and rearranging yields the Doppler shift frequency spectrum:

$$J = J_0 \, \exp \left\{ - \beta^2 \left[\frac{f_D \lambda_0 - \bar{V} \sin\theta}{2 \sin \frac{\theta}{2}} \right]^2 \right\} \tag{10}$$

where J_0 is a new constant.

It can be seen from Eq. 10 that one can obtain the mean flow velocity $\bar{V}$ from the experimental data as follows:

$$\bar{V} = \frac{(f_D)_{peak} \, \lambda_0}{\sin \theta} \tag{11}$$

where $(f_D)_{peak}$ is the Doppler shift frequency at the peak spectral intensity.

The value of β can be obtained by plotting the logarithm (to base 10) of the spectral intensity J as a function of $[f_D \lambda_0 - \bar{V} \sin \theta]^2 / 4 \sin^2 (\theta/2)$. From Eq. 10 it can be

seen that this plot should result in a straight line the
negative slope of which is $\beta^2/2.303$:

$$\beta = \sqrt{2.303 \ (-slope)} \qquad\qquad (12)$$

RESULTS

A sketch of the measured Doppler shift frequency
spectrum, showing the calibration lines, is presented in
Fig. 1. The curve is observed to display the Gaussian shape
predicted by Eq. 10. The peak intensity is found to occur
at a Doppler shift frequency of 8.8 megacyles. From Eq. 11,
this corresponds to a mean flow velocity $\overline{V}$ of 33.7 m/sec.
This value agrees very closely with the value of 35.3 m/sec
obtained by a pitot tube measurement.

The value of β in Eq. 10 was found by plotting in
Fig. 2 the logarithm (to base 10) of the spectral intensity
obtained from Fig. 1 as a function of the parameter

$$[f_D \ \lambda_o - \overline{V} \ \sin \theta]^2/4 \ \sin^2 \ (\theta/2).$$

The straight line fit was found by the method of least
squares. The value of β was determined from Eq. 12 and
utilized in Eq. 6, along with the previously determined

value of mean flow velocity $\bar{V}$, to obtain a turbulence intensity value T of 13.4 percent.

DISCUSSION OF RESULTS

The mean flow velocity determined from the peak intensity of the Doppler shift frequency spectrum is in excellent agreement with the velocity measured by pitot tube. This would leave little doubt as to the utility of the optical Doppler shift method in measuring mean flow velocities in turbulent flows.

No corresponding measurements were made with which to compare the turbulence intensity value of 13.4 percent. A number of factors, however, could conceivably contribute to increased broadening of the Doppler shift frequency spectrum. The measurements reported herein were taken over a time period of one minute. Any variation in the flow during this time would broaden the measured spectrum. Also, no account was made in the analysis for multiple scattering. Furthermore, any vibration in the optical system could contribute to the measured Doppler shift frequency. It is considered that any of these possible errors, however, could be held below acceptable limits through further refinement of the method. Some error can, of course, be caused by slip between the smoke particle velocity and the continuum fluid velocity.

CONCLUSIONS AND RECOMMENDATIONS

1. The measurement of flow velocities in a turbulent gas
   stream can in principle be accomplished accurately
   through use of optical Doppler shift frequency measure-
   ments.

2. It is recommended that comparisons be made of turbulence
   measurements using this method and measurements using
   other existing methods such as hot wire anemometers.

3. The scale of turbulence can be measured much the same
   way as in hot wire techniques in which the velocity
   correlation factor is determined as a function of dis-
   tance between two measuring points. Two separate
   velocity measuring systems are required. Due to
   physical size of the laser beam equipment it is probable
   that small traversing mirrors would be required for
   moving one measuring beam system relative to the other.

REFERENCES

1. Kennard, E.H., Kinetic Theory of Gases, McGraw-Hill
   Book Company, New York (1938) p. 58.

2. Yen, Y. and Cummins, H., App. Phys. Lett. 4, 176 (1964).

3. Hinze, J.O., Turbulence, McGraw-Hill Book Company, New
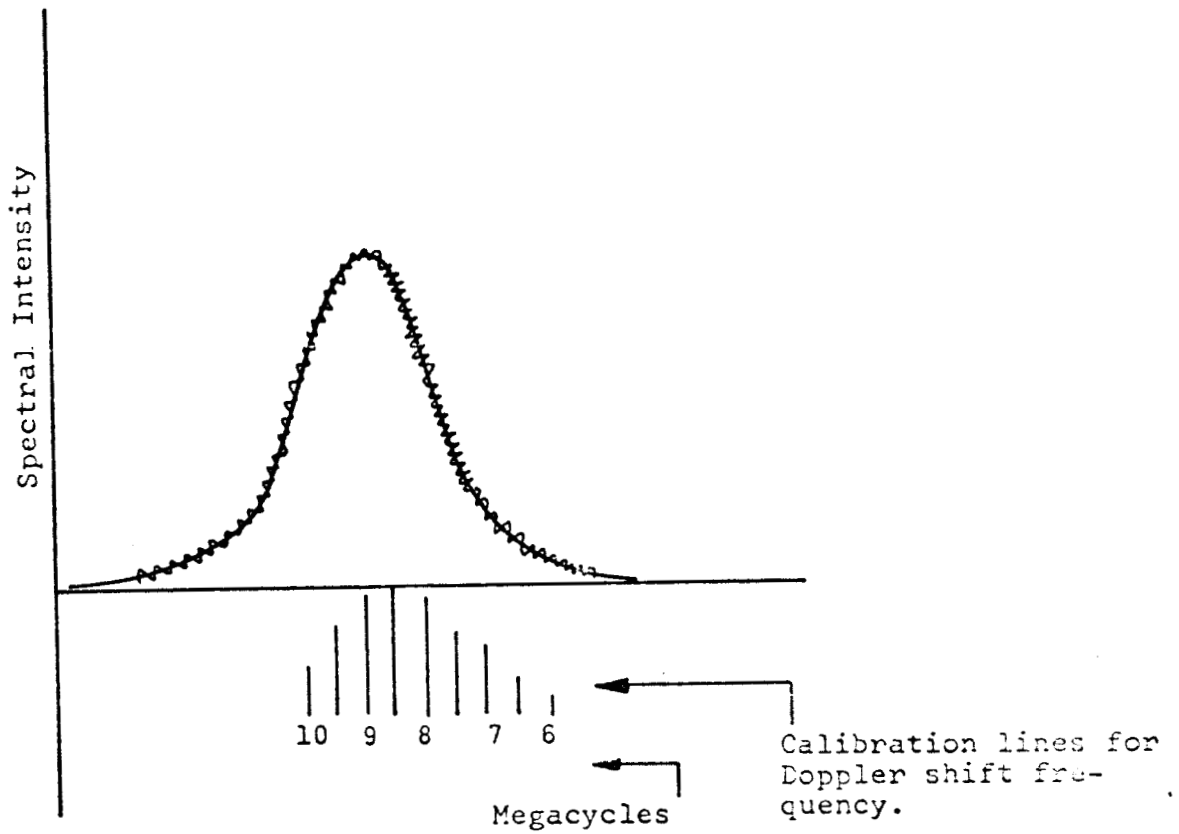   York (1959) p. 4.

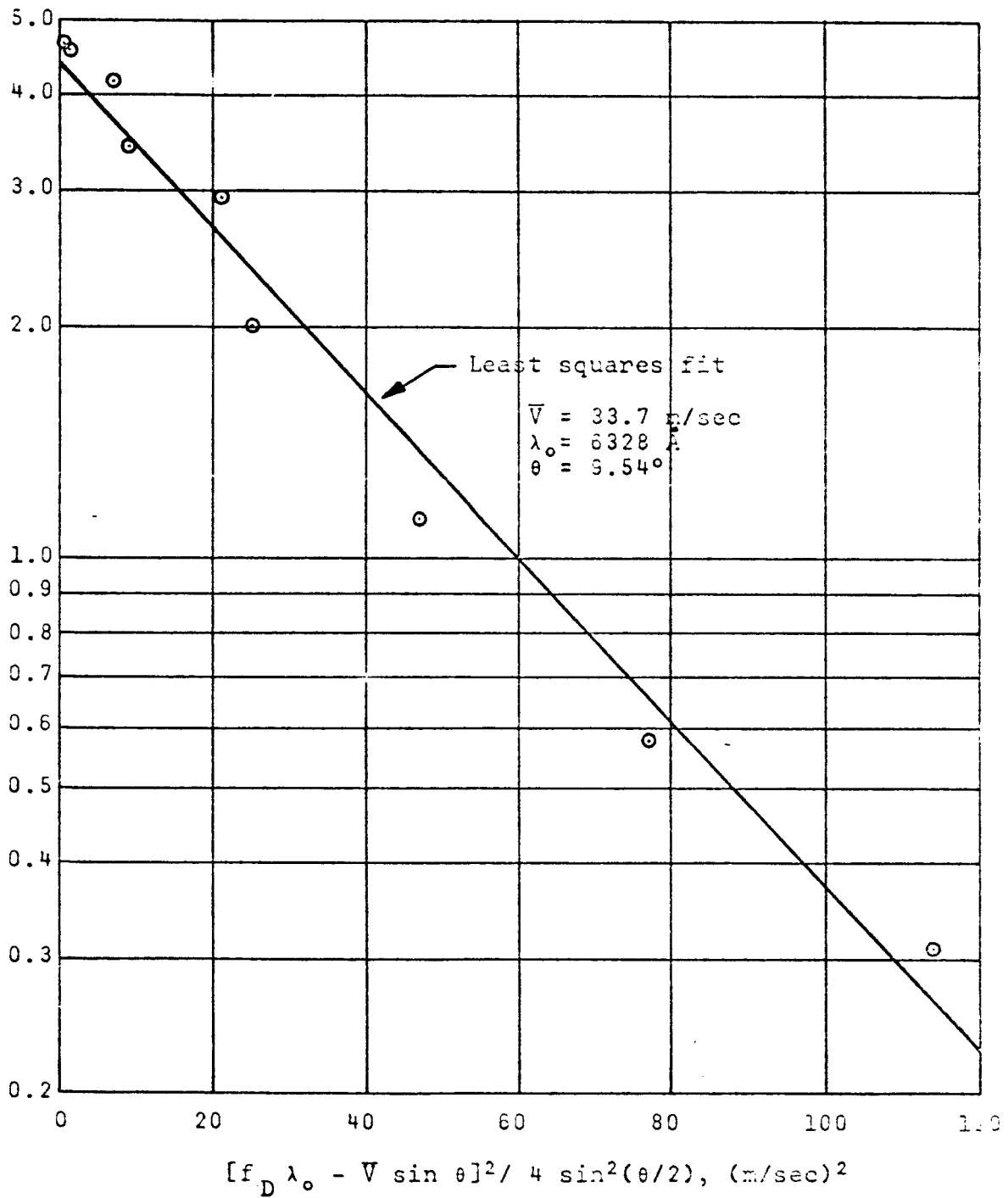Fig. 1 - Sketch of Raw Data Showing Doppler Shift
Frequency Spectrum

Fig. 2 - Log Spectral Intensity J as a Function of

Parameter $[f_D \lambda_o - \bar{V} \sin \theta]^2/4 \sin^2(\theta/2)$

PART VII

IMPORTANCE OF TURBULENCE

INTENSITY ON THE BASE

HEATING PROBLEM

By

Howard Yen

INTRODUCTION

The flow field in the base region of multi-engined rocket vehicles is complex and no satisfactory mathematical model has been presented that will adequately describe the flow field. Recent results of base region turbulence intensity experiments (Ref. 1) show that a high degree of turbulence intensity may exist when the model is experiencing supersonic flow. It is known that the degree of turbulence intensity affects the convective heat transfer rate.

W.V.R. Malkus has developed a theory of turbulent shear flow (Ref. 2) and heat transport of thermal turbulence (Ref. 3). The possible application of these theories to regions of separated flow has been discussed by Hanson and Richardson (Ref. 4). Richardson (Ref. 5) developed an empirical equation similar to Malkus' results to predict the heat transfer coefficient in a separated flow region. The effect of turbulence intensity has been included in Richardson's results by introducing the critical Reynolds number into the equation. The purpose of the present study is to make some evaluation of the applicability of Malkus' theory and Richardson's proposal to the prediction of base heat transfer.

DISCUSSION

Determination of Critical Reynolds Number

<u>Theoretical Determination of Critical Reynolds Number</u>. -
The critical Reynolds number may be determined theoretically
for flows experiencing small perturbations by means of the
Orr-Sommerfeld equation (Ref. 6). The results of calculations
based on the Orr-Sommerfeld equation are shown in the sketch
below (Ref. 7) for a two-dimensional boundary layer having
a two-dimensional disturbance.
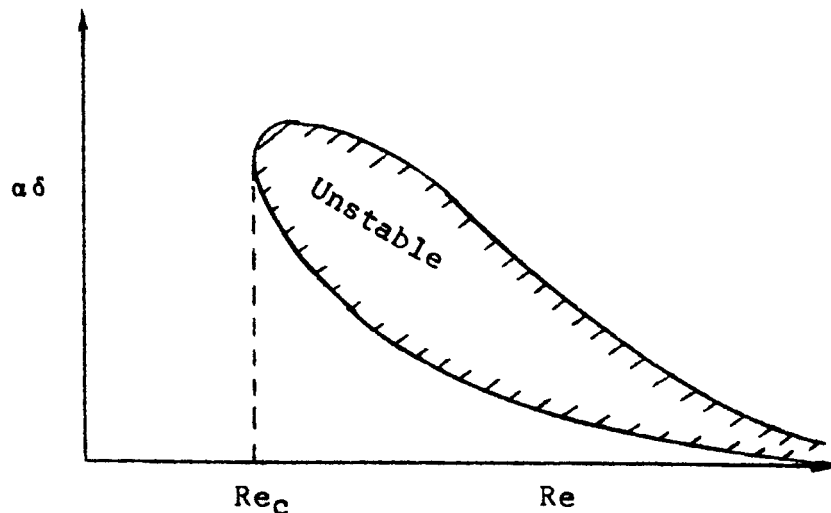
The symbols used in the sketch are defined as follows:

Re = Reynolds number

Re_c = Critical Reynolds number

α = A quantity related to the wavelength of
disturbance by $\lambda = 2\pi/\alpha$

δ = Boundary layer thickness

λ = Wavelength of disturbance.

Reference to the above sketch shows that the smallest unstable Reynolds number is the critical Reynolds number. The critical Reynolds number for flow over a flat plate has been determined to be approximately 420 (Ref. 7).

Experimental Determination of Critical Reynolds Number. - Laminar to turbulent boundary layer transition measurements have been performed by several investigators who have found that the transitional Reynolds number may be described as a function of the following nondimensional parameters (Ref. 9):

$$(Re)_t = \left(\frac{U\delta}{\nu}\right)_t = F\left(\frac{\delta^2}{\nu}\frac{dU}{dx}, \frac{\delta}{r}, \frac{\epsilon}{\delta}, \frac{L}{\delta}, \frac{u'}{U}\right) \tag{1}$$

where $(Re)_t$ is the transitional Reynolds number, U is the free stream velocity, δ is the boundary layer thickness, ν is the kinematic viscosity, dU/dx is related to the pressure gradient, r is the radius of curvature, ϵ is the surface roughness, L is the scale of turbulence, and u'/U is the turbulence intensity.

No satisfactory function has been obtained which will completely define the experimental critical Reynolds number. An experimentally determined critical Reynolds number for flow over a flat plate with a moderately small turbulence intensity is $Re_x = 3 \times 10^5$ where the subscript x refers to the wetted length. Conversion of the characteristic length from wetted length to boundary layer displacement thickness

gives a critical Reynolds number of $Re_{\delta*} = 950$ (Ref. 8)
compared to the theoretically determined value of 420.
Instrumentation response time prevents the determination
of the initial flow disturbances and is believed to be the
major factor causing the discrepancy between the theoretical
and experimental values of critical Reynolds number.

Methods of Heat Transfer Prediction by

Malkus' Theory and Richardson's Correlation

Malkus' Theoretical Results. - Malkus' results of heat
transport by turbulent, fully developed free convection between
two parallel flat plates can be stated as

$$H/(\rho_o C_v) = K \beta_o \left(\frac{Ra}{Ra_c}\right)^{1/3} \qquad (2)$$

where H is the heat transport, ρ_o is the average density, C_v
is the specific heat capacity, K is the thermometric conductivity,
β_o is the negative temperature gradient between the plates, Ra
is the Rayleigh number, and Ra_c is the critical Rayleigh number.
By using the definition of the Nusselt number, Eq. (2) may be
rewritten as

$$Nu = \left(\frac{Ra}{Ra_c}\right)^{1/3} . \qquad (3)$$

Richardson's Experimental Results. - Richardson (Ref. 5) observed results of an experiment involving heat transfer from the rear of a body immersed in a uniform flow to the region of separated flow. It was found that the results were correlated well by an equation of the form

$$Nu = A \ Re^{2/3} \ Pr^{1/3}. \tag{4}$$

In determination of the constant A, Richardson related his results to Malkus' results by a concept of "paradox flow". He found that the forced convection in separated flow is similar to free convection between two horizontal parallel plates (Ref. 5). Taking the form of Malkus' results (Eq. 3), Richardson found that the constant A may be related to the critical Reynolds number by an equation of the form

$$A = \left(\frac{1}{Re_c}\right)^{2/3}. \tag{5}$$

Eq. (4) can, therefore, be rewritten as

$$Nu = \left(\frac{Re}{Re_c}\right)^{2/3} Pr^{1/3}. \tag{6}$$

Richardson demonstrated that Eq. (6) conformed fairly well with experimental data.

Influence of Turbulence Intensity

on Convective Heat Transfer

For extremely low turbulence intensities of the order of $T < 0.001$, the critical Reynolds number can be increased to 3×10^6 for flat plate flow compared to a critical Reynolds number of 3×10^5 at moderate turbulence intensities. It is known that the degree of turbulence intensity affects the critical Reynolds number on flows other than classical flat plate flows. From Eq. (6) the change of critical Reynolds number will strongly affect the heat transfer rate. In recent results of base regime turbulence intensity experiments reported by Ref. 1, turbulence intensities of 40 to 100 percent have been observed; therefore, it is evident that the effect of turbulence intensity on convective heat transfer can not be neglected in the base heating problem.

CONCLUSIONS

The Orr-Sommerfeld equation for instability is not applicable to the problem of determining critical Reynolds numbers in the base region of test models experiencing flow with large values of turbulence intensities. Turbulence intensities as high as 40 to 100 percent have been observed on the base of test models experiencing supersonic flows.

Richardson's correlation is shown to be an empirical

equation which relates convective heat transfer and critical

Reynolds number.

REFERENCES

1. R. E. Larson et al., "Base Heating and Separation Studies", Contract NAS8-11299, Eighth Monthly Progress Report, Litton Systems, Inc., Applied Science Division, 1965.

2. W.V.R. Malkus, "Outline of a Theory of Turbulent Shear Flow", J. Fluid Mechanics, Vol. 2, 1957, pp. 521-539.

3. W.V.R. Malkus, "The Heat Transport and Spectrum of Thermal Turbulence", Proc. Roy. Soc., Ser. A., Vol. 225, pp. 196-212, 1954.

4. F.B. Hanson and P.D. Richardson, "Mechanics of Turbulent Separated Flow as Indicated by Heat Transfer: A Review", ASME Symposium on Fully Separated Flow, May 1964.

5. P.D. Richardson, "Estimation of the Heat Transfer from the Rear of an Immersed Body to the Region of Separated Flow", Aeronautical Research Laboratories Report No. ARL 62-423, USAF, Sept. 1962.

6. H. Schlichting, Boundary Layer Theory, Fourth Edition, McGraw-Hill Book Company, New York, 1960, Chapt. 16.

7. Ibid., p. 397.

8. Ibid., p. 125.

9. H. L. Dryden, "Transition from Laminar to Turbulent Flow", Turbulent Flows and Heat Transfer, Princeton University Press, 1959, pp. 19-21.